

C3a and suPAR drive versican V1 expression in tubular cells of focal segmental glomerulosclerosis

Runhong Han,^{1,2} Shuai Hu,² Weisong Qin,² Jinsong Shi,² Qin Hou,² Xia Wang,² Xiaodong Xu,² Minchao Zhang,² Caihong Zeng,² Zhihong Liu,^{1,2} and Hao Bao^{1,2}

¹Southeast University School of Medicine, National Clinical Research Center of Kidney Diseases, Jinling Hospital, Nanjing, China. ²National Clinical Research Center of Kidney Diseases, Jinling Hospital, Nanjing University School of Medicine, Nanjing, China.

Chronic tubulointerstitial injury impacts the prognosis of focal segmental glomerulosclerosis (FSGS). We found that the level of versican V1 was increased in tubular cells of FSGS patients. Tubular cell-derived versican V1 induced proliferation and collagen synthesis by activating the CD44/Smad3 pathway in fibroblasts. Both urine C3a and suPAR were increased and bound to the tubular cells in FSGS patients. C3a promoted the transcription of versican by activating the AKT/ β -catenin pathway. C3aR knockout decreased the expression of versican in Adriamycin-treated (ADR-treated) mice. On the other hand, suPAR bound to integrin β 6 and activated Rac1, which bound to SRp40 at the 5' end of exon 7 in versican pre-mRNA. This binding inhibited the 3'-end splicing of intron 6 and the base-pair interactions between intron 6 and intron 8, leading to the formation of versican V1. Cotreatment with ADR and suPAR specifically increased the level of versican V1 in tubulointerstitial tissues and caused more obvious interstitial fibrosis in mice than treatment with only ADR. Altogether, our results show that C3a and suPAR drive versican V1 expression in tubular cells by promoting transcription and splicing, respectively, and the increases in tubular cell-derived versican V1 induce interstitial fibrosis by activating fibroblasts in FSGS.

Introduction

Focal segmental glomerulosclerosis (FSGS) accounts for 40% of cases of nephrotic syndrome in adults (1). Severe tubulointerstitial fibrosis is an independent risk factor of renal function decline in patients with FSGS (2, 3). We completed a transcriptome analysis of tubulointerstitial tissues from FSGS patients and normal controls. The level of versican V1 was increased in the tubulointerstitial tissues and had the most significant relationship with the estimated glomerular filtration rate (eGFR) decline rate in FSGS patients. Versican is a large extracellular matrix proteoglycan that is present in a variety of human tissues. Bukong et al. reported that versican expression increased during liver fibrosis (4). Rienstra et al. showed that versican expression was dominant during renal fibrosis in an experimental renal transplantation rat model (5).

During nephrotic syndrome, plasma protein leakage into the urinary space contributes directly to local tissue injury. Deposits of the complement component 3 (C3) protein were detected on the proximal tubules of kidneys from nephrotic patients (6). We noted that the level of C3 mRNA was also increased in the tubulointerstitial tissues and was related to the eGFR decline rate in FSGS patients. Therefore, both systemic and local complement synthesis contribute to intrarenal complement activation. Other factors, such as soluble urokinase-type plasminogen activator receptor (suPAR), have been linked to renal disease, first as a potential circulating bioactive factor causing FSGS and then as a predictor of the rate of chronic kidney disease progression (7, 8). In patients with FSGS, the urinary excretion of suPAR was increased and was associated with disease severity (9).

Based on our findings, we believe that the increase in versican V1 may be associated with the abnormal exposure of renal tubular cells to leaked plasma proteins in FSGS patients. In this study, experiments were conducted to investigate the underlying mechanism of versican V1 overexpression in tubular cells and the role of versican V1 in renal fibrosis in FSGS patients.

Authorship note: RH and SH are co-first authors.

Conflict of interest: The authors have declared that no conflict of interest exists.

Copyright: © 2019 American Society for Clinical Investigation

Submitted: June 14, 2018

Accepted: February 14, 2019

Published: April 4, 2019.

Reference information: *JCI Insight*. 2019;4(7):e122912. <https://doi.org/10.1172/jci.insight.122912>.

Results

Versican V1 mRNA expression in renal tubulointerstitial tissues predicts the renal function decline rate in FSGS patients. Renal tubulointerstitial tissues from FSGS patients and controls were microdissected under a stereomicroscope, and an Affymetrix HTA 2.0 microarray was used to perform a global analysis of the gene expression patterns in the tissues (Figure 1A and Supplemental Table 1; supplemental material available online with this article; <https://doi.org/10.1172/jci.insight.122912DS1>). Among the differentially expressed genes, the level of versican mRNA showed the highest correlation coefficient with the eGFR decline rate (Figure 1B and Supplemental Table 2). Reverse transcription PCR (RT-PCR) analysis confirmed that the level of total versican mRNA was significantly increased in the tubulointerstitial tissues of FSGS patients (Figure 1, C and D).

Three versican isoforms, V0, V1, and V3, exist in renal tissues (10). RT-PCR analysis showed that the level of versican V1, but not the V0 or V3 isoform, was increased in the tubulointerstitial tissues of FSGS patients (Figure 1D). Versican V1 mRNA expression was significantly correlated with the serum creatinine level, interstitial fibrosis score, and eGFR decline rate in FSGS patients (Figure 1, E–G). Western blot analysis confirmed that the level of versican V1, but not V0, was increased in the tubulointerstitial tissues of FSGS patients (Figure 1H). Immunohistochemical staining showed that versican V1 was upregulated in renal tubular cells and accumulated in the interstitium of patients with FSGS (Figure 1, I and J).

Tubular cell–derived versican V1 induces proliferation and collagen synthesis in renal fibroblasts. Human renal tubular cells were cultured and treated in vitro. The overexpression of versican V1 did not increase the level of collagen I (Col I) in tubular cells (Figure 2, A and B). Instead, the secretion of versican V1 was significantly increased in the medium of tubular cells overexpressing versican V1 (Figure 2C).

Renal fibroblasts are located adjacent to tubular cells in the renal anatomy. The conditioned medium of tubular cells was collected and added to renal fibroblasts. The conditioned medium of tubular cells overexpressing versican V1 significantly induced proliferation and collagen synthesis in fibroblasts (Figure 2, D and E). To confirm the effect of versican V1 on fibroblasts, we produced His-tagged human versican V1 in tubular cells and purified it on a Ni-chelate column. Treatment with purified versican V1 significantly induced proliferation and collagen synthesis in fibroblasts. Comparatively, treatment with versican V0 induced only a slight increase in proliferation and collagen synthesis in fibroblasts, and treatment with versican V3 failed to induce proliferation and collagen synthesis in fibroblasts (Figure 2, F and G).

Versican can bind to the surface proteins CD44, ITGB1, EGFR, and PSGL1 (11). Silencing CD44 but not ITGB1, EGFR, or PSGL1 prevented proliferation and collagen synthesis in fibroblasts treated with versican V1 (Figure 2, H and I). Immunoprecipitation and Western blot analyses showed that versican V1 bound to CD44 and activated Smad3 in fibroblasts (Figure 2, J and K). Treatment with a CD44 mAb or silencing Smad3 decreased proliferation and collagen synthesis in fibroblasts treated with versican V1 (Figure 2, L–O).

Overexpression of versican V1 in tubular cells induces renal interstitial fibrosis in mice. The overexpression of versican V1 in tubular cells via the hydrodynamic-based delivery of a versican V1–expressing plasmid caused the accumulation of versican V1 in the renal interstitium of mice (Figure 3, A–C). Immunoprecipitation analysis showed that the binding between versican V1 and CD44 was increased in the tubulointerstitial tissues of mice overexpressing versican V1 (Figure 3D). The overexpression of versican V1 induced the phosphorylation of Smad3 in the tubulointerstitial tissues of mice (Figure 3E). The accumulation of fibroblasts and the level of Col I in tubulointerstitial tissues were obviously increased in the mice overexpressing versican V1 (Figure 3, F–H). As a result, mice overexpressing versican V1 showed increased serum creatinine levels and obvious interstitial fibrosis (Figure 3, I–K). Treatment with CD44 mAb prevented the binding between versican V1 and CD44, decreased the phosphorylation of Smad3, inhibited the accumulation of fibroblasts and collagen synthesis in the tubulointerstitial tissues, and suppressed interstitial fibrosis in the mice overexpressing versican V1.

C3a promotes the transcription of versican by activating the AKT/ β -catenin pathway in tubular cells. Abnormal exposure to patient or healthy serum samples increased the level of versican mRNA in tubular cells, and this effect was abolished in cells treated with heat-inactivated serum (Figure 4A). Blocking studies showed that the inhibition of C3aR but not C5b-9 prevented the increase in versican in tubular cells treated with patient serum (Figure 4B). The levels of both serum and urine C3a were increased in patients with FSGS (Figure 4, C and D). Immunofluorescence analysis showed that C3a bound to C3aR on the apical surface of the renal tubular cells in patients with FSGS (Figure 4E).

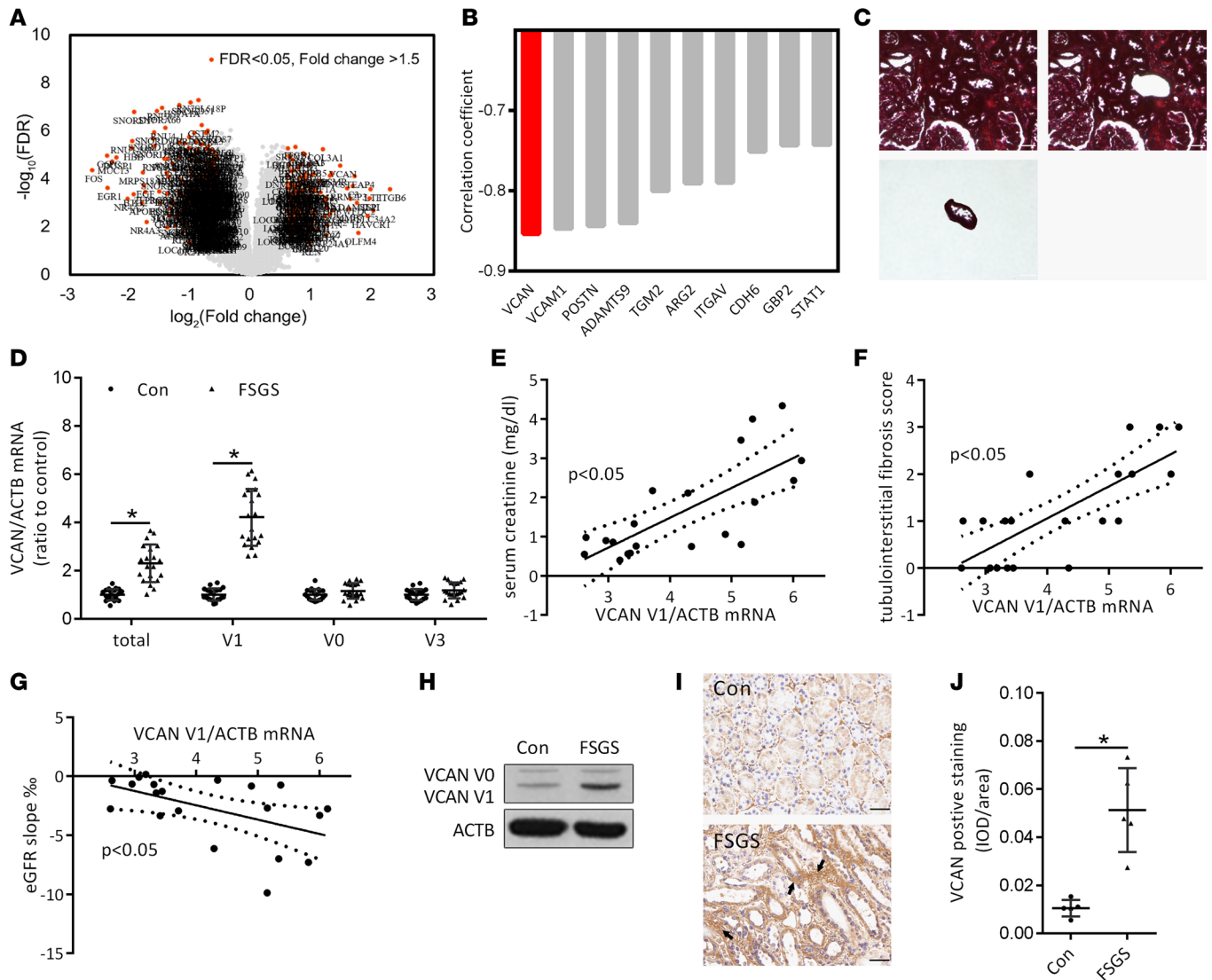


Figure 1. Expression of versican V1 in renal tubulointerstitial tissues of FSGS patients. (A) Volcano plot of differentially expressed genes in tubulointerstitial tissues of FSGS patients with cutoff values of fold change >1.5 and FDR <0.05 ($n = 8$). (B) Correlation between the level of differentially expressed genes and eGFR decline rate in FSGS patients ($n = 8$). (C) Isolation of tubulointerstitial tissues by laser capture microdissection. Scale bar: 20 μm . (D) RT-PCR analysis of total versican, versican V1, V0, and V3 levels in tubulointerstitial tissues of FSGS patients and controls (Con) ($n = 20$). (E–G) Correlation between the level of versican V1 mRNA and the level of serum creatinine, tubulointerstitial fibrosis score, or eGFR decline rate in FSGS patients ($n = 20$). (H) Western blot analysis of versican V1 and V0 in tubulointerstitial tissues of FSGS patients and normal control ($n = 3$). (I and J) Immunohistochemical analysis of versican in FSGS patients and normal controls ($n = 5$). Arrows indicate that versican V1 was expressed in renal tubular cells and accumulated in the interstitium of patients with FSGS. Scale bars: 20 μm . For statistical analysis, a 2-tailed Student's t test was used for D and J, Pearson's correlation was used for E and G, and Spearman's correlation was used for F. * $P < 0.05$ compared with control.

Treatment with C3a alone sufficiently induced the overexpression of versican in tubular cells (Figure 4F). Interestingly, although the level of total versican was comparable between the cells treated with patient serum and those treated with C3a, treatment with patient serum specifically induced the expression of versican V1. C3a treatment, however, increased the expression of all versican isoforms, suggesting that C3a promotes versican transcription in tubular cells.

Protein kinase B (AKT), p38, and extracellular signal-regulated kinase (ERK) function downstream of C3aR (12–15). The AKT inhibitor MK2206 but not the p38 inhibitor SB203580 or the ERK inhibitor PD098059 significantly prevented the upregulation of versican in tubular cells treated with C3a (Figure 5, A and B). Treatment with C3a induced the phosphorylation of AKT in tubular cells, and this effect was prevented by a C3aR antagonist (Figure 5C).

The versican promoter was predicted to be regulated by TCF transcription factors, and AKT can

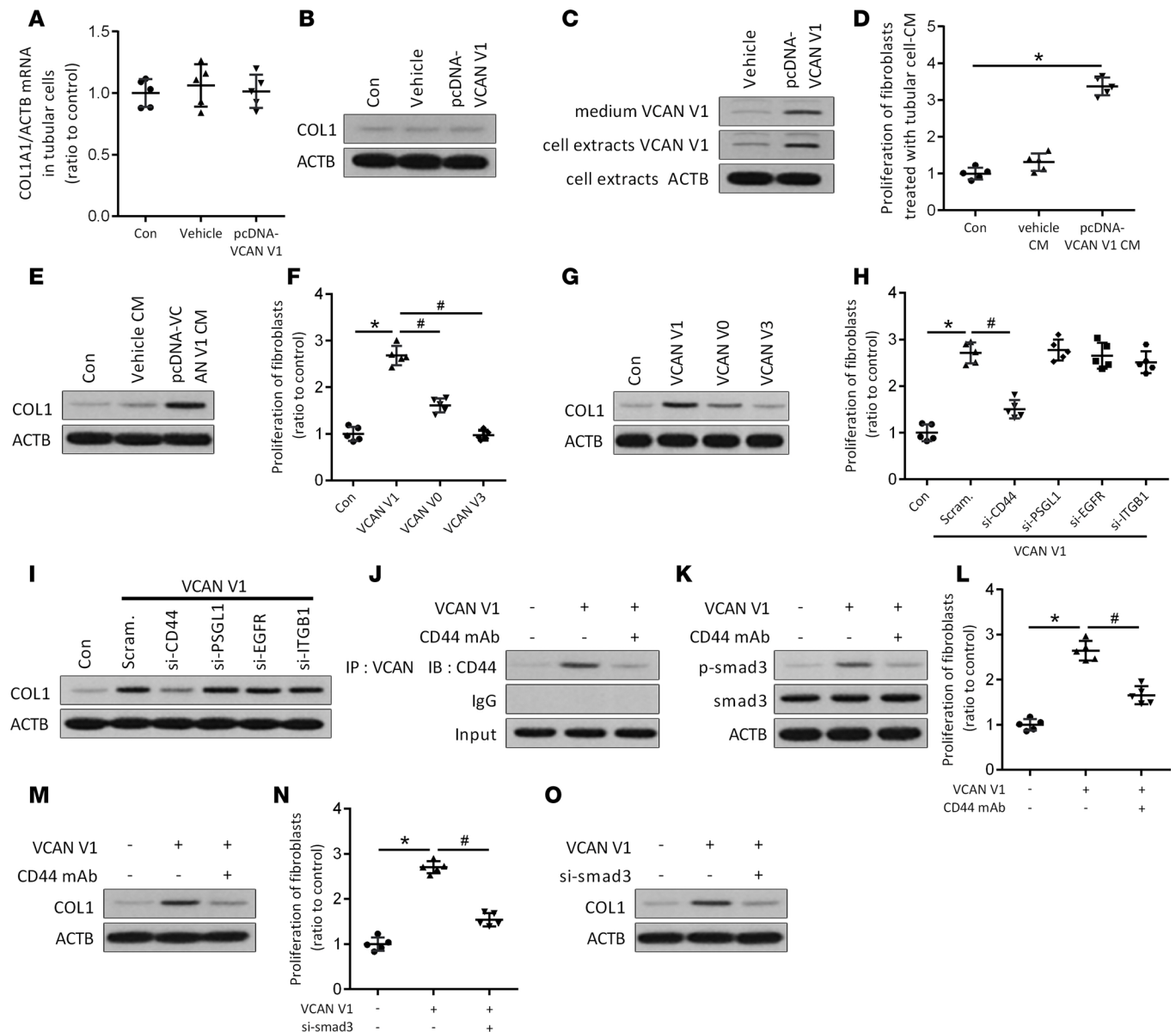


Figure 2. Effect of tubular cell-derived versican V1 on fibrogenic activation of renal fibroblasts. (A) RT-PCR analysis of collagen I (Col I) in tubular cells transfected with versican V1 plasmid ($n = 5$). (B) Western blot analysis of Col I in tubular cells transfected with versican V1 plasmid ($n = 3$). (C) Western blot analysis of versican V1 in the cell extracts and culture medium of tubular cells transfected with versican V1 plasmid ($n = 3$). (D) BrdU cell proliferation analysis of renal fibroblasts treated with the conditioned medium of versican V1-overexpressing tubular cells (pcDNA-VCAN V1 CM) ($n = 5$). (E) Western blot analysis of Col I in renal fibroblasts treated with the conditioned medium of versican V1-overexpressing tubular cells ($n = 3$). (F) BrdU cell proliferation analysis of renal fibroblasts treated with purified versican V1, V0, or V3 ($n = 5$). (G) Western blot analysis of Col I in renal fibroblasts treated with purified versican V1, V0, or V3 ($n = 3$). (H) BrdU cell proliferation analysis of renal fibroblasts treated with versican V1, si-CD44, si-PSGL1, si-EGFR, or si-ITGB1 ($n = 5$). (I) Western blot analysis of Col I in renal fibroblasts treated with versican V1, si-CD44, si-PSGL1, si-EGFR, or si-ITGB1 ($n = 3$). (J) IP analysis of the binding between versican and CD44 in renal fibroblasts treated with versican V1 and CD44 mAb ($n = 3$). (K) Western blot analysis of p-Smad3 in renal fibroblasts treated with versican V1 and CD44 mAb ($n = 3$). (L) BrdU cell proliferation analysis of renal fibroblasts treated with versican V1 and CD44 mAb ($n = 5$). (M) Western blot analysis of Col I in renal fibroblasts treated with versican V1 and CD44 mAb ($n = 3$). (N) BrdU cell proliferation analysis of renal fibroblasts treated with versican V1 and si-Smad3 ($n = 5$). (O) Western blot analysis of Col I in renal fibroblasts treated with versican V1 and si-Smad3 ($n = 3$). For statistical analysis, 1-way ANOVA with Tukey's post hoc test was used for A, D, F, H, L, and N. * $P < 0.05$ compared with control; # $P < 0.05$ compared with renal fibroblasts treated with versican V1.

activate β -catenin/TCF transcriptional activity by the indirect stabilization of β -catenin and the direct phosphorylation of β -catenin. Nuclear β -catenin was increased in tubular cells treated with C3a, and the inhibition of AKT prevented the C3a-induced translocation of β -catenin (Figure 5D).

ChIP analysis showed that β -catenin bound to the versican promoter in tubular cells, and this effect was enhanced by C3a treatment (Figure 5, E and F). The overexpression of a constitutively active form

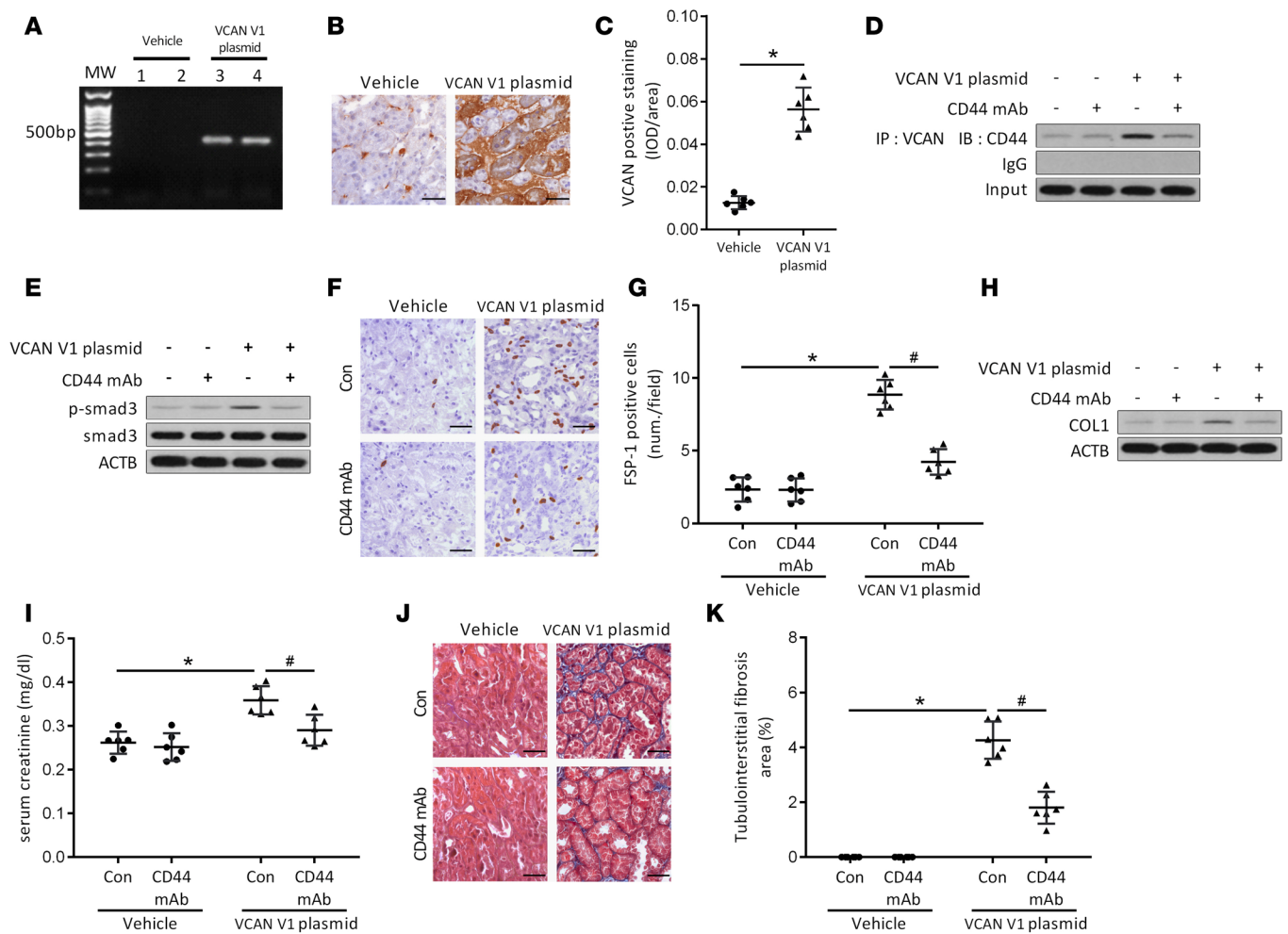


Figure 3. Effect of versican V1 overexpression on tubulointerstitial fibrosis in mice. (A) PCR analysis of pcDNA-versican V1 sequence in tubulointerstitial tissues of mice treated with control plasmid or versican V1-expressing plasmid (VCAN V1 plasmid). (B and C) Immunohistochemical analysis of versican V1 in tubulointerstitial tissues of mice ($n = 6$). (D) IP analysis of the binding between versican V1 and CD44 in tubulointerstitial tissues of mice treated with VCAN V1 plasmid and CD44 mAb ($n = 6$). (E) Western blot analysis of p-Smad3 in tubulointerstitial tissues of mice ($n = 6$). (F and G) Immunohistochemical analysis of renal fibroblasts in tubulointerstitial tissues of mice ($n = 6$). (H) Western blot analysis of Col I in tubulointerstitial tissues of mice ($n = 6$). (I) Level of serum creatinine in mice ($n = 6$). (J and K) Masson's trichrome staining of renal sections of mice ($n = 6$). Scale bars: 20 μm (B, F, and J). For statistical analysis, a 2-tailed Student's t test was used for C, and 1-way ANOVA with Tukey's post hoc test was used for G, I, and K. * $P < 0.05$ compared with mice treated with control plasmid; # $P < 0.05$ compared with mice treated with VCAN V1 plasmid.

of β -catenin (N90- β -catenin) increased the expression of the luciferase reporter construct containing the binding sequence. Site-directed mutations rescued the β -catenin-mediated upregulation of the versican promoter-luciferase reporter plasmid (Figure 5G). β -Catenin overexpression also increased endogenous versican expression (Figure 5H). Conversely, β -catenin knockdown suppressed C3a-induced versican expression in tubular cells (Figure 5I).

C3aR knockout prevents the upregulation of versican in the tubular cells of ADR-treated mice. Treatment with ADR caused an obvious increase in serum creatinine levels and renal interstitial fibrosis in WT mice (Figure 6, A–C). The levels of all versican isoforms were significantly increased in the tubulointerstitial tissues of WT mice treated with ADR (Figure 6D). Immunohistochemical staining showed that the expression of versican was upregulated in the tubular cells of ADR-treated mice (Figure 6, E and F).

Although a significant increase in urinary C3a was observed in both ADR-treated WT and C3aR-knockout mice, C3aR knockout abolished the deposition of C3a on the tubular cells of ADR-treated mice (Figure 6, G and H). C3aR knockout also suppressed the phosphorylation of AKT, attenuated the nuclear accumulation of β -catenin, and decreased the interaction between β -catenin and the promoter region of versican in the tubulointerstitial tissues of ADR-treated mice (Figure 6, I–K).

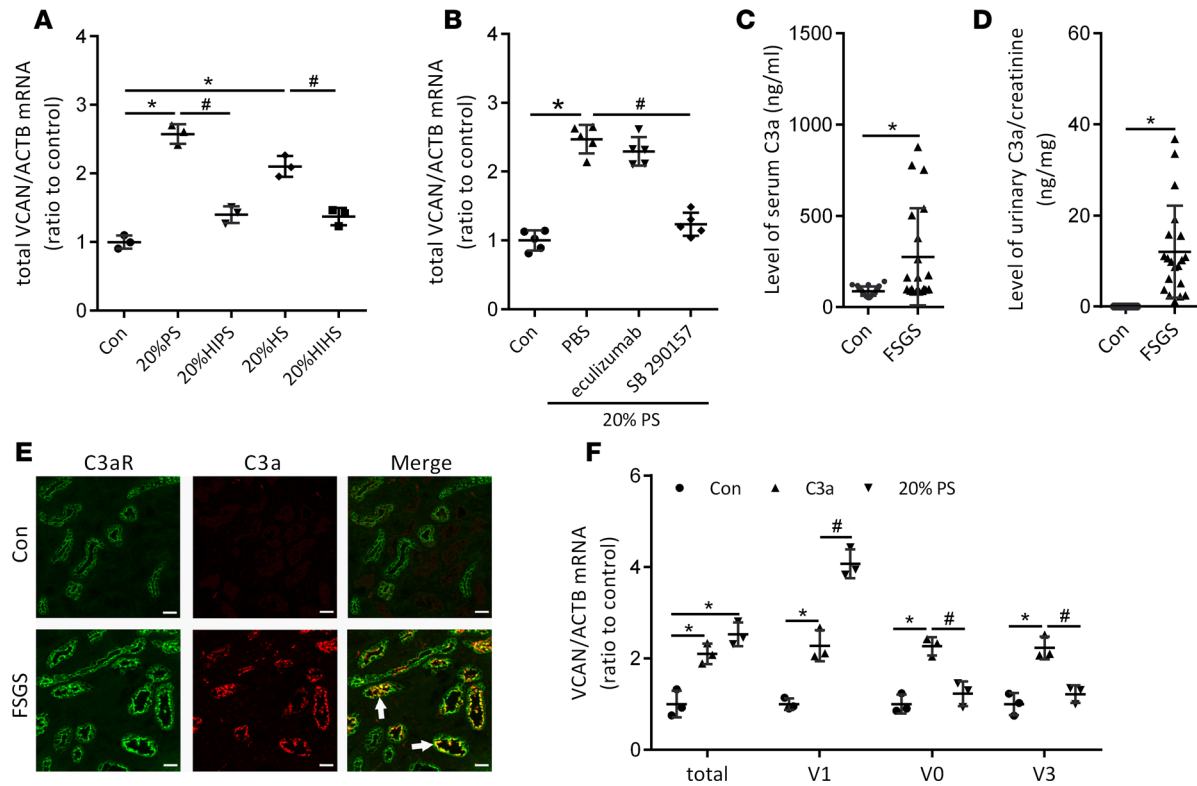


Figure 4. C3a induces versican expression in tubular cells of FSGS. (A) RT-PCR analysis of total versican in tubular cells treated with 20% patient serum (PS), 20% heat-inactivated patient serum (HIPS), 20% healthy serum (HS), or 20% heat-inactivated healthy serum (HIHS) for 48 hours ($n = 3$). (B) RT-PCR analysis of total versican in tubular cells treated with 20% PS, eculizumab, or SB290157 for 48 hours ($n = 5$). (C) Level of serum C3a in FSGS patients and controls ($n = 20$). (D) Level of urinary C3a in FSGS patients and controls ($n = 20$). (E) Immunofluorescence staining of C3a (red) and C3aR (green) in renal tissue of FSGS patients ($n = 3$). (F) RT-PCR analysis of total versican, versican V1, V0, and V3 in tubular cells treated with C3a or 20% PS for 48 hours ($n = 3$). Scale bars: 20 μm . For statistical analysis, 1-way ANOVA with Tukey's post hoc test was used for A, B, and F, and a 2-tailed Student's t test was used for C and D. * $P < 0.05$ compared with control; # $P < 0.05$ compared with PS-, HS-, or C3a-treated cells.

As a result, the expression of versican was decreased in the tubulointerstitial tissues of C3aR-knockout mice treated with ADR (Figure 6, E and L).

suPAR regulates the alternative splicing of versican pre-mRNA by activating the $\beta 6$ -integrin/Rac1 pathway in tubular cells. suPAR is a circulating molecule that has been shown to be associated with renal function decline in renal disease. Both the serum levels and urine excretion of suPAR were increased in FSGS patients (Figure 7, A and B). Immunohistochemical analysis revealed a high level of suPAR binding to the tubular cells of FSGS patients (Figure 7C). Blocking studies showed that the inhibition of suPAR decreased the level of versican V1 and increased the levels of versican V0 and V3 in tubular cells treated with patient serum, but the level of total versican mRNA was not affected (Figure 7D). In contrast to the upregulation of all versican isoforms in cells treated with C3a alone, the expression of versican V1 was specifically increased in cells that were treated with the combination of C3a and suPAR, which mimicked the effect of patient serum (Figure 7E).

suPAR binds to $\beta 3$ integrin and activates the Rac1 pathway in podocytes (16, 17). Among the integrin β subunits, integrin $\beta 6$ (ITGB6) showed the greatest increase in FSGS patients in our transcriptome analysis. RT-PCR analysis confirmed that the level of ITGB6 was increased in the tubulointerstitial tissues of FSGS patients (Figure 7F). suPAR interacted directly with ITGB6 in tubular cells treated with patient serum (Figure 7, G and H). Treatment with ITGB6 siRNA decreased the level of versican V1 and increased the levels of versican V0 and V3 in the tubular cells treated with patient serum (Figure 7I).

Treatment with patient serum led to an obvious activation of Rac1 in the tubular cells, and this effect was prevented by ITGB6 siRNA (Figure 7J). Silencing Rac1 decreased the level of versican V1 and increased the levels of versican V0 and V3 in tubular cells treated with patient serum, and this was similar to the effect of ITGB6 siRNA (Figure 7K).

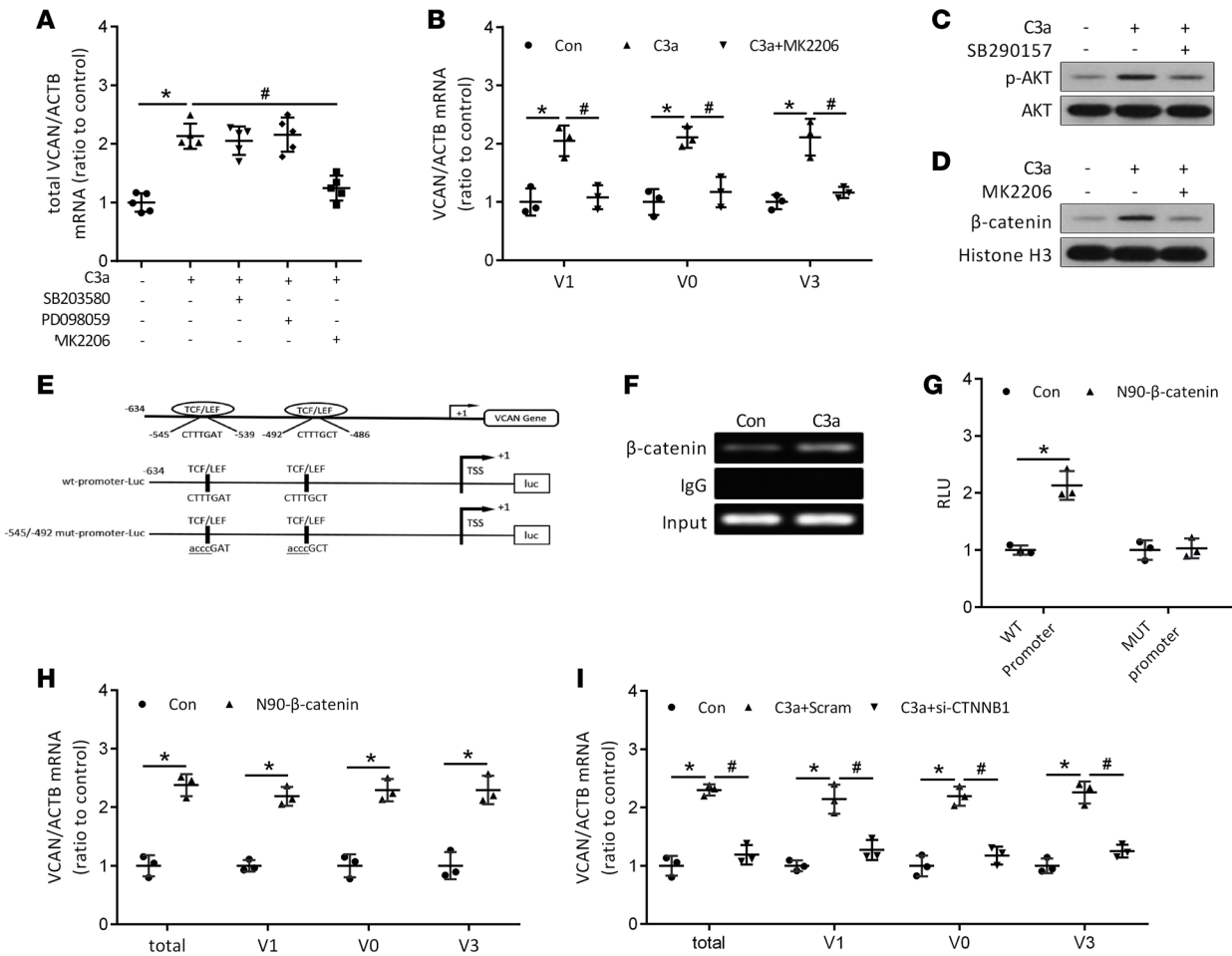


Figure 5. C3a induces versican expression by activating the AKT/β-catenin pathway in tubular cells. (A) RT-PCR analysis of total versican in tubular cells treated with C3a and SB203580, PD098059, or MK2206 ($n = 5$). (B) RT-PCR analysis of versican V1, V0, and V3 in tubular cells treated with C3a and MK2206 ($n = 3$). (C) Western blot analysis of phospho-AKT (p-AKT) in tubular cells ($n = 3$). (D) Western blot analysis of nuclear β-catenin in tubular cells ($n = 3$). (E) Schematic of the β-catenin/TCF binding sites in the upstream sequence of the versican promoter and the constructed versican promoter-luciferase reporter plasmids. (F) ChIP analysis of the binding between β-catenin and the versican promoter in tubular cells treated with C3a ($n = 3$). (G) Normalized luciferase activity of reporter constructs in tubular cells cotransfected with N90-β-catenin plasmid ($n = 3$). (H) RT-PCR analysis of total versican, versican V1, V0, and V3 in tubular cells transfected with N90-β-catenin plasmid ($n = 3$). (I) RT-PCR analysis of total versican, versican V1, V0, and V3 in tubular cells treated with C3a and si-CTNNB1 ($n = 3$). For statistical analysis, 1-way ANOVA with Tukey's post hoc test was used for A, B, and I, and a 2-tailed Student's t test was used for G and H. * $P < 0.05$ compared with control; # $P < 0.05$ compared with C3a-treated cells.

Rac1 induces the skipping of versican exon 7 by interacting with SRp40 in tubular cells. We explored splicing factors with the SpliceAid 2 database (18). Some splicing factors were predicted to bind to the 5' end of versican exon 7 (Figure 8A). Among them, immunoprecipitation analysis showed that Rac1 bound to SRp40 in tubular cells, and this binding was enhanced by treatment with patient serum (Figure 8B). Immunofluorescence staining confirmed that Rac1 colocalized with SRp40 in the nuclei of tubular cells treated with patient serum (Figure 8C).

Both Rac1 and SRp40 bound to the 5' end of versican exon 7 in the serum-treated tubular cells (Figure 8D). Silencing SRp40 decreased the binding between Rac1 and the 5' end of exon 7 of versican pre-mRNA, but silencing Rac1 did not affect the binding between SRp40 and the 5' end of exon 7 of versican pre-mRNA (Figure 8, E and F). Treatment with SRp40 siRNA did not change the Rac1 activity in serum-treated tubular cells (Figure 8G). The differential effects of Rac1 siRNA and SRp40 siRNA indicated that the binding between Rac1 and the 5' end of exon 7 of versican pre-mRNA is mediated by SRp40 in tubular cells.

The SRp40 protein increases the binding of the U2 small nuclear ribonucleoprotein auxiliary factor to an upstream 3' splice site via binding to the exon (19). In serum-treated tubular cells,

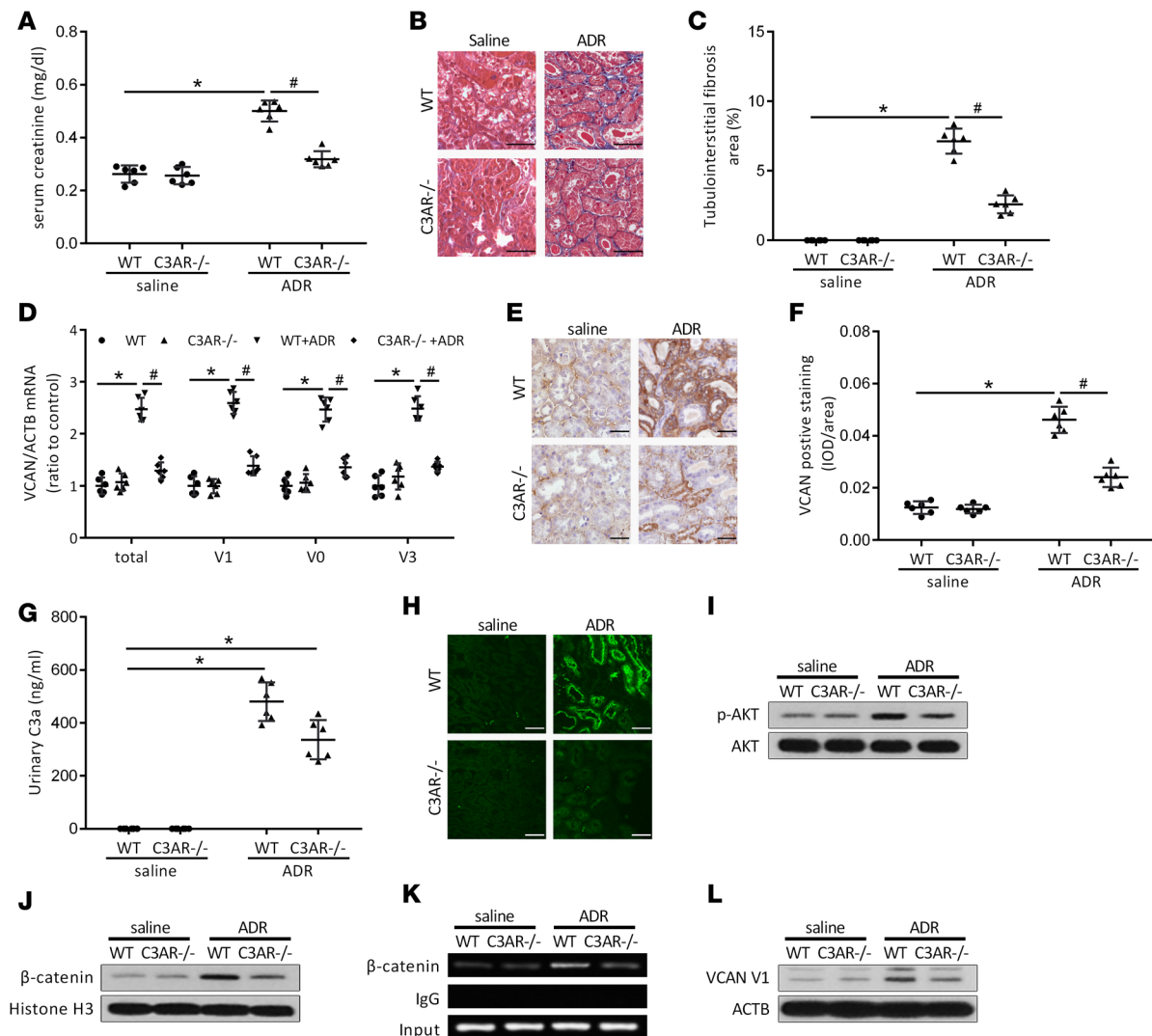


Figure 6. Effect of C3aR knockout on the expression of versican in tubular cells of ADR-treated mice. (A) Level of serum creatinine in WT and C3aR-knockout (C3aR^{-/-}) mice treated with Adriamycin (ADR) ($n = 6$). (B and C) Masson's trichrome staining of renal sections in WT and C3aR^{-/-} mice treated with ADR ($n = 6$). (D) RT-PCR analysis of total versican, versican V1, V0, and V3 in tubulointerstitial tissues of WT and C3aR^{-/-} mice treated with ADR ($n = 6$). (E and F) Immunohistochemical staining of versican in renal tissues of WT and C3aR^{-/-} mice treated with ADR ($n = 6$). (G) Level of urinary C3a in WT and C3aR^{-/-} mice treated with ADR ($n = 6$). (H) Immunofluorescence staining of C3a in WT and C3aR^{-/-} mice treated with ADR ($n = 6$). (I) Western blot analysis of p-AKT in tubulointerstitial tissues of WT and C3aR^{-/-} mice treated with ADR ($n = 6$). (J) Western blot analysis of nuclear β-catenin ($n = 6$). (K) ChIP analysis of the binding between β-catenin and the versican promoter in tubulointerstitial tissues ($n = 6$). (L) Western blot analysis of versican V1 in tubulointerstitial tissues ($n = 6$). Scale bars: 20 μm (E and H). Scale bars: 30 μm (B). For statistical analysis, 1-way ANOVA with Tukey's post hoc test was used for A, C, D, F, and G. * $P < 0.05$ compared with control WT mice; # $P < 0.05$ compared with ADR-treated WT mice.

although the transcription of versican pre-mRNA was upregulated, the binding between U2AF1 and the 3' splice site of intron 6 in versican pre-mRNA was suppressed, and the level of versican V0 was not increased. SRp40 overexpression or blocking suPAR rescued the splicing inhibition at the 3' splice site of intron 6, which increased the level of versican V0 in the serum-treated tubular cells (Figure 8, H and I). Conversely, although C3a increased both versican V0 and V1 levels in tubular cells, Rac1^{Q61L} overexpression or cotreatment with suPAR suppressed the binding between U2AF1 and the 3' splice site of intron 6 in versican pre-mRNA and specifically increased the level of versican V1 in C3a-treated tubular cells (Figure 8, J and K).

Rac1 prevents the formation of versican V3 by interfering with the intron 6 and 8 interaction in versican pre-mRNA in tubular cells. Sequence scanning revealed that a 34-nt complementary sequence exists at intron 6 (site 1) and intron 8 (site 2) of versican pre-mRNA (Figure 9A). Such an interaction may

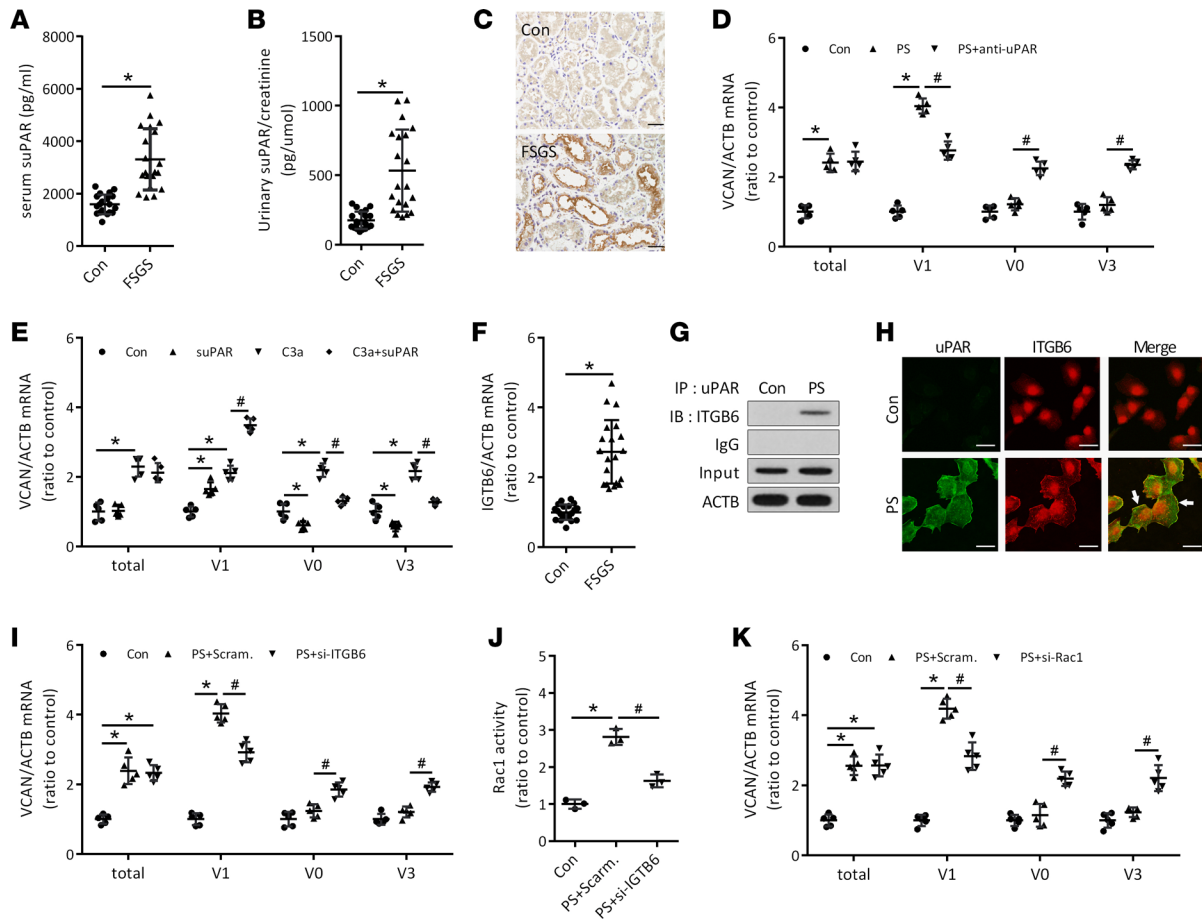


Figure 7. Effect of suPAR on the alternative splicing of versican pre-mRNA in tubular cells. (A) Level of serum suPAR in FSGS patients ($n = 20$). (B) Level of urinary suPAR in FSGS patients ($n = 20$). (C) Immunohistochemical staining of uPAR in renal tissues of FSGS patients ($n = 5$). (D) RT-PCR analysis of total versican, versican V1, V0, and V3 in tubular cells treated with 20% PS and uPAR-blocking antibody ($n = 5$). (E) RT-PCR analysis of total versican, versican V1, V0, and V3 in tubular cells treated with C3a and suPAR ($n = 5$). (F) RT-PCR analysis of ITGB6 in tubulointerstitial tissues of FSGS patients ($n = 20$). (G) IP analysis of the binding between suPAR and ITGB6 in tubular cells treated with 20% PS ($n = 3$). (H) Immunofluorescence staining of uPAR (green) and ITGB6 (red) in tubular cells treated with 20% PS ($n = 3$). Scale bars: 20 μm (C and H). (I) RT-PCR analysis of total versican, versican V1, V0, and V3 in tubular cells treated with 20% PS and si-ITGB6 ($n = 5$). (J) Rac1 activation assay in tubular cells treated with 20% PS and si-ITGB6 ($n = 3$). (K) RT-PCR analysis of total versican, versican V1, V0, and V3 in tubular cells treated with 20% PS and si-Rac1 ($n = 5$). For statistical analysis, a 2-tailed Student's t test was used for A, B, and F, and 1-way ANOVA with Tukey's post hoc test was used for D, E, I, J, and K. * $P < 0.05$ compared with control; # $P < 0.05$ compared with PS- or C3a-treated cells.

lead to the formation of a stem-loop structure and the exclusion of exon 7 and exon 8 from versican mRNA. RAP analysis confirmed that site 1 at intron 6 bound directly to site 2 at intron 8 of versican pre-mRNA (Figure 9B). Treatment with locked nucleic acid (LNA) antisense oligonucleotides targeting either site 1 or site 2 prevented the intron 6/8 interaction and decreased the level of versican V3 mRNA in the tubular cells (Figure 9, C and D).

The complementary sequence of intron 6 is located 7 nucleotides away from the binding site of Rac1/SRp40. The overexpression of constitutively active Rac1^{Q61L} decreased the intron 6/8 interaction in versican pre-mRNA and decreased the level of versican V3 in tubular cells (Figure 9, E and F). Treatment with SRp40 siRNA restored the intron 6/8 interaction and increased the level of versican V3 in tubular cells overexpressing Rac1^{Q61L}.

Although treatment with patient serum did not increase the intron 6/8 interaction or the expression of versican V3 in tubular cells, patient serum significantly increased the intron 6/8 interaction and the expression of versican V3 in tubular cells treated with Rac1 siRNA or an anti-suPAR antibody (Figure 9, G and H). Inversely, treatment with C3a directly increased the intron 6/8 interaction and the expression of versican V3 in tubular cells, and these effects were prevented by the overexpression of Rac1^{Q61L} or cotreatment with suPAR (Figure 9, I and J).

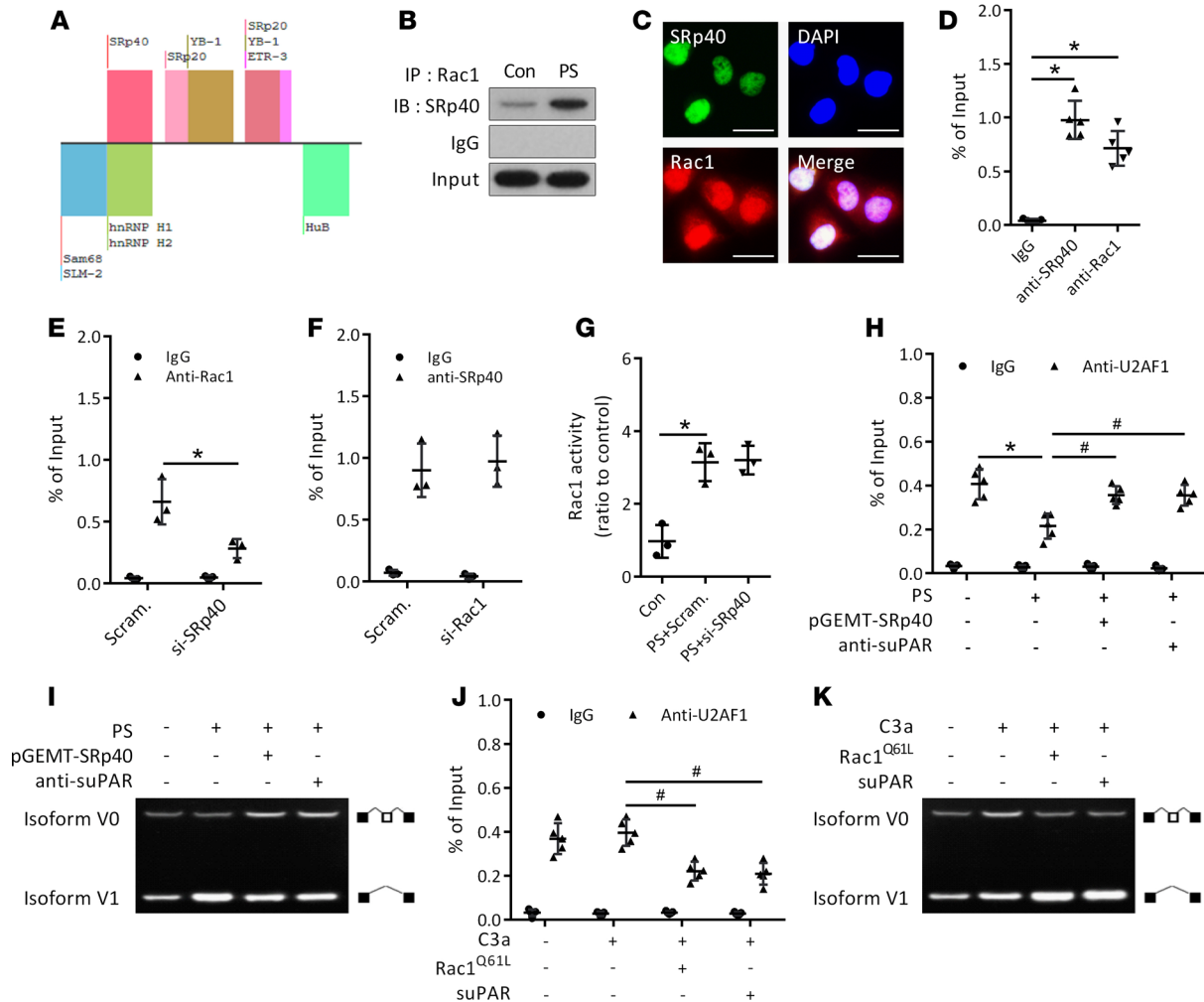


Figure 8. Rac1 induces the skipping of versican exon 7 by interacting with SRp40 in tubular cells. (A) Splicing factors predicted to bind to the 5' end of versican exon 7 with the SpliceAid 2 database. (B) IP analysis of the binding between Rac1 and SRp40 in tubular cells treated with 20% PS ($n = 3$). (C) Immunofluorescence staining of SRp40 (green), Rac1 (red), and DAPI (blue) in tubular cells treated with 20% PS ($n = 3$). Scale bars: 20 μm . (D) RIP analysis of the binding of Rac1 to the 5' end of versican exon 7 in tubular cells treated with 20% PS and si-SRp40 ($n = 3$). (E) RIP analysis of the binding of Rac1 to the 5' end of versican exon 7 in tubular cells treated with 20% PS and si-SRp40 ($n = 3$). (F) RIP analysis of the binding of SRp40 to the 5' end of versican exon 7 in tubular cells treated with 20% PS and si-Rac1 ($n = 3$). (G) Rac1 activity in tubular cells treated with 20% PS and si-SRp40 ($n = 3$). (H) RIP analysis of the binding of U2AF1 to the 3' splice site of versican intron 6 in tubular cells treated with 20% PS and pGEMT-SRp40 plasmid or suPAR-blocking antibody ($n = 5$). (I) PCR analysis of versican V0 and V1 in tubular cells treated with 20% PS and pGEMT-SRp40 plasmid or suPAR-blocking antibody ($n = 3$). (J) RIP analysis of the binding of U2AF1 to the 3' splice site of versican intron 6 in tubular cells treated with C3a and Rac1^{Q61L} plasmid or suPAR ($n = 5$). (K) PCR analysis of versican V0 and V1 in tubular cells treated with C3a and Rac1^{Q61L} plasmid or suPAR ($n = 3$). For statistical analysis, 1-way ANOVA with Tukey's post hoc test was used for D-F, G, H, and J. * $P < 0.05$ compared with control; # $P < 0.05$ compared with PS- or C3a-treated cells.

suPAR regulates the alternative splicing of versican pre-mRNA in the tubular cells of ADR-treated mice. The binding sequence of Rac1/SRp40 is conserved at the 5' end of exon 7 in mouse versican pre-mRNA, and importantly, the matching motifs of intron 6 and intron 8 are also present in the mouse versican pre-mRNA sequence (Figure 10A).

Treatment with ADR alone did not increase the urine suPAR levels or activate Rac1 in the tubulointerstitial tissues of mice (Figure 10, B–E). The binding of Rac1 to SRp40 or to the 5' end of versican exon 7 was not increased in the tubulointerstitial tissues of ADR-treated mice (Figure 10, F and G). As a result, treatment with ADR increased all versican isoforms in the tubulointerstitial tissues of mice (Figure 10, H–J).

suPAR could not pass freely through the normal glomerular filtration barrier (20). The injection of suPAR alone did not increase the urine excretion of suPAR in normal mice; however, cotreatment with ADR and suPAR significantly increased the urinary excretion of suPAR, and a considerable amount

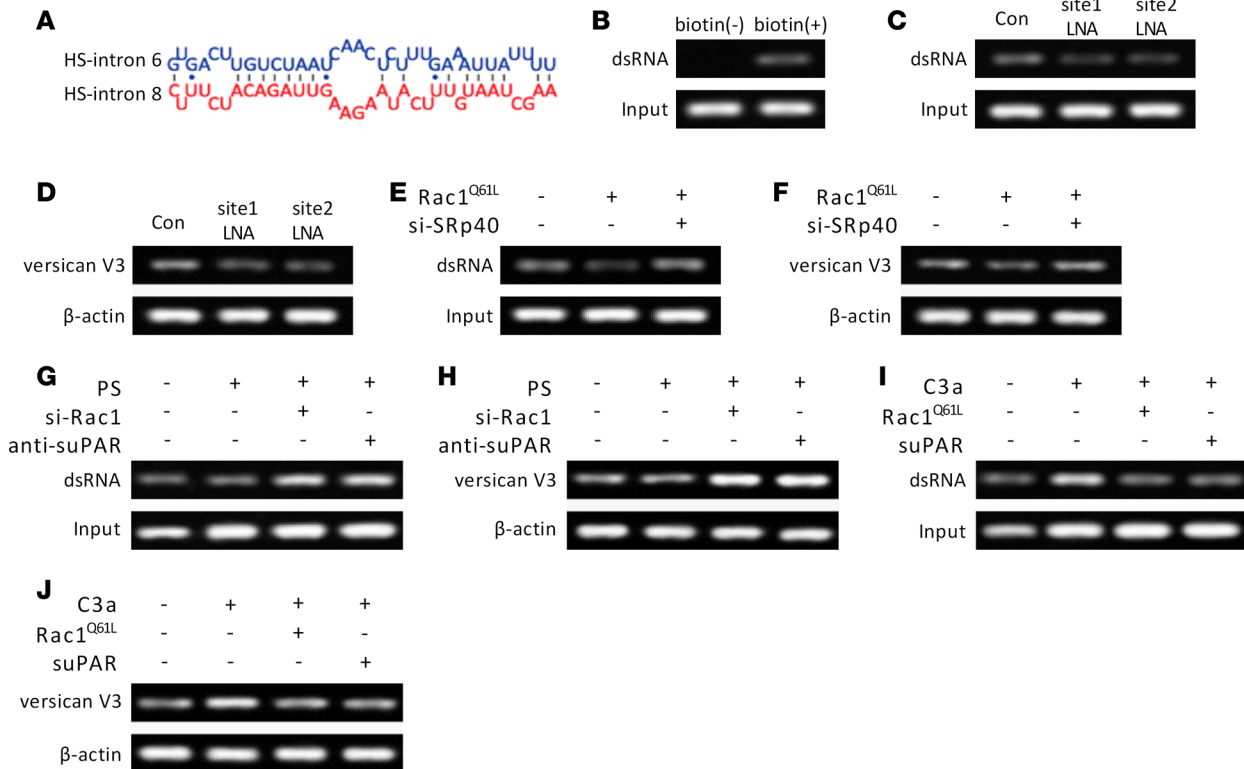


Figure 9. Rac1 prevents the formation of versican V3 by interfering with the intron 6/8 interaction in versican pre-mRNA of tubular cells. (A) Model of the 34-nt complementary sequence in intron 6 (site 1) and intron 8 (site 2) of versican pre-mRNA. (B) RAP analysis of the intron 6/8 interaction in versican pre-mRNA of tubular cells ($n = 3$). (C) RAP analysis of the intron 6/8 interaction in versican pre-mRNA of tubular cells treated with LNA antisense oligonucleotides targeting either site 1 or site 2 ($n = 3$). (D) PCR analysis of versican V3 in tubular cells ($n = 3$). (E) RAP analysis of the intron 6/8 interaction in versican pre-mRNA of tubular cells transfected with Rac1^{O61L} plasmid and si-SRp40 ($n = 3$). (F) PCR analysis of versican V3 in tubular cells transfected with Rac1^{O61L} plasmid and si-SRp40 ($n = 3$). (G) RAP analysis of the intron 6/8 interaction in versican pre-mRNA of tubular cells treated with 20% PS and si-Rac1 or suPAR-blocking antibody ($n = 3$). (H) PCR analysis of versican V3 in tubular cells treated with 20% PS and si-Rac1 or suPAR-blocking antibody ($n = 3$). (I) RAP analysis of the intron 6/8 interaction in versican pre-mRNA of tubular cells treated with C3a and Rac1^{O61L} plasmid or suPAR ($n = 3$). (J) PCR analysis of versican V3 in tubular cells treated with C3a and Rac1^{O61L} plasmid or suPAR ($n = 3$).

of suPAR bound to the renal tubular cells (Figure 10, B and C). Cotreatment with ADR and suPAR induced the activation and nuclear translocation of Rac1, which led to an increase in the interaction between Rac1 and SRp40 in renal tubulointerstitial tissues (Figure 10, D–F). The binding between Rac1 and the 5' end of versican exon 7 was increased, and the interaction between intron 6 and intron 8 was blunted in the tubulointerstitial tissues of mice treated with both ADR and suPAR (Figure 10, G and H). Cotreatment with ADR and suPAR specifically increased the level of versican V1 in the tubulointerstitial tissues (Figure 10, I and J). The binding between versican V1 and CD44 and the phosphorylation of Smad3 were greater in the tubulointerstitial tissues of mice treated with ADR and suPAR than in those of mice treated with only ADR (Figure 10, K and L). As a result, compared with ADR treatment alone, cotreatment with ADR and suPAR aggravated the accumulation of fibroblasts and collagen synthesis and caused higher serum creatinine levels and more obvious interstitial fibrosis in mice (Figure 10, M–R).

Discussion

In this study, we found that the level of versican V1 was increased in tubulointerstitial tissues and was related to the eGFR decline rate in FSGS patients. Versican is an extracellular matrix protein belonging to a family of hyaluronan-binding proteoglycans. It is a major component of the fibroproliferative matrix in hepatic fibrosis and lung fibrosis (4, 21). Consistent with our findings, Einecke et al. evaluated the gene expression in 105 transplanted renal biopsies and found that versican was one of the most significantly upregulated genes and predicted renal graft loss in kidney transplantation (22). Rudnicki et al. evaluated the level of versican mRNA in 74 renal biopsies and found that increased renal versican expression was associated with the progression of chronic kidney disease (10).

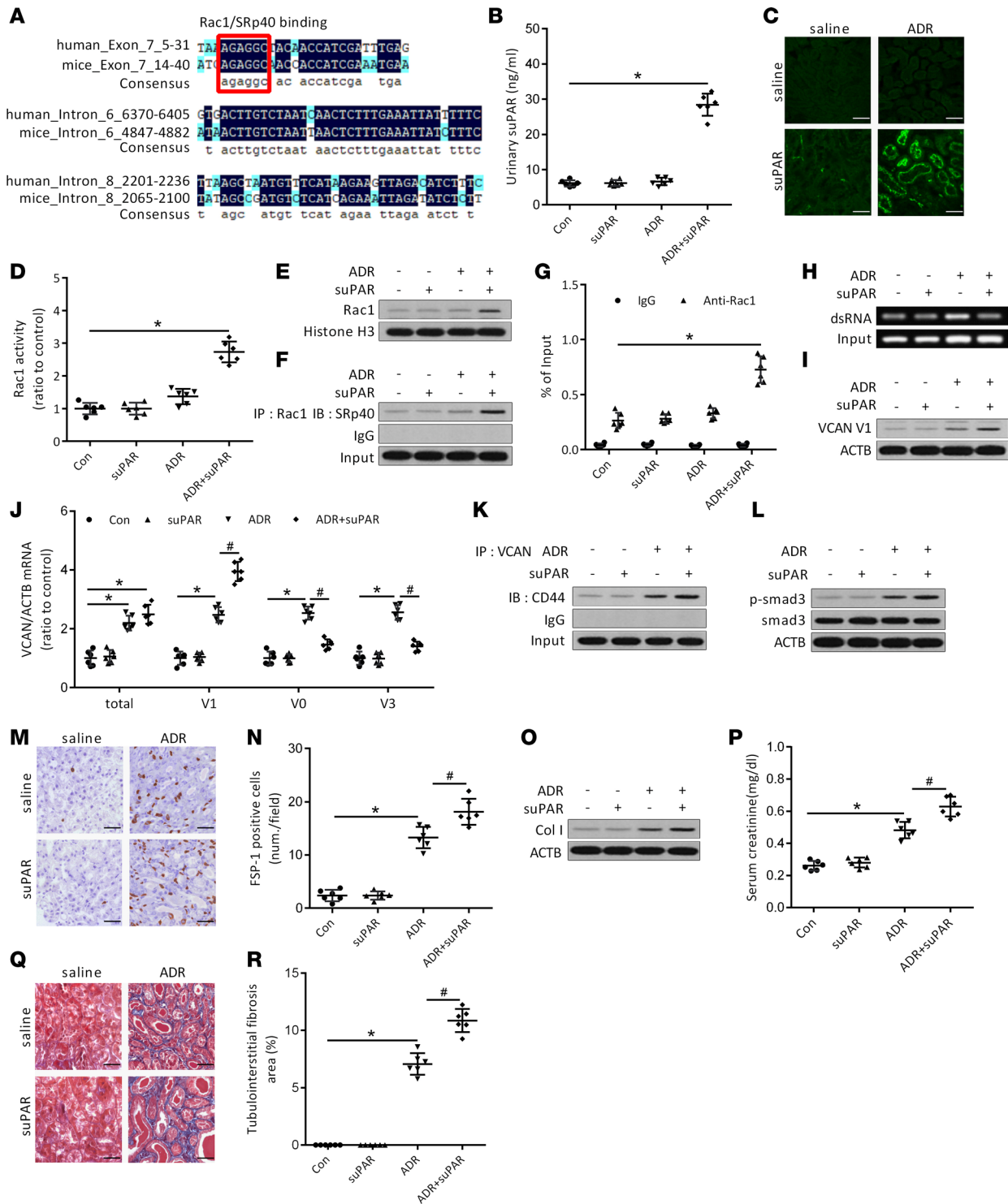


Figure 10. Effect of suPAR on the alternative splicing of versican pre-mRNA in tubular cells of ADR-treated mice. (A) Sequence alignment of versican exon 7, intron 6 (site 1) and intron 8 (site 2) between human and mouse. (B) Level of urinary suPAR in ADR- and suPAR-treated mice ($n = 6$). (C) Immunofluorescence staining of suPAR in renal tissues of mice treated with ADR and suPAR ($n = 6$). (D) Rac1 activation assay in tubulointerstitial tissues ($n = 6$). (E) Western blot analysis of nuclear Rac1 in tubulointerstitial tissues ($n = 6$). (F) IP analysis of the binding between Rac1 and SRp40 in tubulointerstitial tissues ($n = 6$). (G) RIP analysis of the binding of Rac1 to the 5' end of versican exon 7 in tubulointerstitial tissues ($n = 6$). (H) RAP analysis of the intron 6/8 interaction in versican pre-mRNA of tubulointerstitial tissues ($n = 6$). (I) Western blot analysis of versican V1 in tubulointerstitial tissues of mice treated with ADR and suPAR ($n = 6$). (J) RT-PCR analysis of total versican, versican V1, V0, and V3 in tubulointerstitial tissues of mice ($n = 6$). (K) IP analysis of the binding between versican and CD44 in tubulointerstitial tissues of mice ($n = 6$). (L) Western blot analysis of p-Smad3 in tubulointerstitial tissues of mice ($n = 6$). (M and N) Immunohistochemical analysis of renal fibroblasts in tubulointerstitial tissues of mice ($n = 6$). (O) Western blot analysis of Col I in tubulointerstitial tissues of mice ($n = 6$). (P) Level of serum creatinine in mice ($n = 6$). (Q and R) Masson's trichrome staining of renal sections in mice ($n = 6$). Scale bars: 20 μ m (C, M, and Q). For statistical analysis, 1-way ANOVA with Tukey's post hoc test was used for B, D, G, J, N, P, and R. * $P < 0.05$ compared with control mice; # $P < 0.05$ compared with ADR-treated mice.

Tubular cell–derived versican V1 bound to CD44 and activated Smad3, which induced cell proliferation and collagen synthesis in renal fibroblasts. The CD44 antigen is a cell-surface glycoprotein involved in cell-cell interactions, cell adhesion, and migration. Roy-Chaudhury et al. showed that CD44 expression was upregulated in focal interstitial infiltrates and within the interstitial fibroblasts and extracellular matrix in FSGS patients (23). Rouschop et al. reported that CD44 deficiency reduces renal fibrosis in obstructive nephropathy (24), and Chen et al. reported that oligo-fucoidan prevents renal tubulointerstitial fibrosis by inhibiting the CD44 signaling pathway (25). We found that versican V1 overexpression in tubular cells induced the accumulation of fibroblasts and interstitial fibrosis in mice, and this effect was prevented by blocking CD44. Consistent with these observations, Li et al. reported that both the invasive phenotype and progressive fibrosis were inhibited in the absence of CD44, and treatment with a CD44-blocking antibody reduced lung fibrosis in mice (26).

Intrarenal complement system activation is involved in the progression of renal disease (27, 28). A key target of the activated complement cascade is the proximal tubule, a site where abnormally filtered plasma proteins and complement factors combine to promote injury (29). Zaferani et al. found that tubular heparan sulfate serves as a docking platform for the alternative complement component properdin in proteinuric renal disease (30). Liu et al. reported that compared with FSGS patients with no or mild tubulointerstitial injury, those with moderate or severe tubulointerstitial injury exhibited a lower level of serum C3 (31). Wang et al. reported that nephrotic syndrome patients with C3 deposition in their renal tubules have more severe disease conditions, tubulointerstitial injury, and recurrence (32). We found that C3a bound to the tubular cells of FSGS patients and that C3a promoted the transcription of versican in tubular cells. Consistent with this, Tang et al. showed that C3a induces tubular epithelial to mesenchymal transition in proteinuric nephropathy (33).

β -Catenin signaling plays an important role in regulating fibrogenic activation. Cai et al. reported that overexpression of the adapter protein FHL2 increased β -catenin dephosphorylation, nuclear translocation, and β -catenin–mediated transcription of snail and vimentin (34). AKT can activate β -catenin/TCF transcriptional activity by the indirect stabilization of β -catenin through GSK-3 β inhibition and by the direct phosphorylation of β -catenin (35). Rahmani et al. reported that versican transcription is mediated by the GSK-3 β pathway via the β -catenin–TCF transcription factor complex in smooth muscle cells (36). We found that treatment with C3a led to an obvious phosphorylation of AKT and the nuclear accumulation of β -catenin in tubular cells, and we confirmed that the increase in nuclear β -catenin caused binding to the promoter region and prompted the expression of versican in the tubular cells of FSGS patients.

Pre-mRNA splicing is a key posttranscriptional regulation process in which introns are excised, and exons are ligated together (37). Previously, Zhao et al. reported that the increased expression of versican isoforms upon TGF- β treatment was greatest for the V0 and V2 isoforms in human trabecular meshwork cells (38). Three versican isoforms, V0, V1, and V3, exist in renal tissues (10, 39). We found that the expression of versican V1 but not versican V0 or V3 was increased in the tubulointerstitial tissues of FSGS patients. The different expression patterns suggest that versican isoforms may have different functions. Sheng et al. reported that the versican V1 isoform enhanced cell proliferation and activated EGFR expression, while the V2 isoform exhibited opposite biological activities by inhibiting cell proliferation and downregulating the expression of EGFR and cyclin A in NIH3T3 fibroblasts (40). Wu et al. reported that the expression of the versican V1 isoform in PC12 cells induced complete differentiation, whereas the expression of V2 induced aborted differentiation accompanied by apoptosis (41). We found that treatment with versican V1 but not versican V0 or V3 obviously induced cell proliferation and collagen synthesis in renal fibroblasts.

suPAR is a glycosylphosphatidyl inositol–anchored (GPI-anchored) 3-domain protein that can be released from the plasma membrane as a soluble molecule by cleavage of the GPI anchor (42, 43). Circulating suPAR has been postulated to cause acute proteinuric kidney disease, specifically FSGS, although the animal models and clinical data in the original reports have been challenged (17, 20, 44). Further studies revealed an inverse correlation between the eGFR and suPAR in FSGS patients (45). A large-cohort study showed that the increased level of suPAR was associated with an accelerated eGFR decline in patients enrolled in the Emory Cardiovascular Biobank (8). The evidence for suPAR as a sensitive biomarker for CKD progression is currently strong, but the underlying mechanism remains unexplained (46). We found that suPAR regulates the alternative splicing of versican pre-mRNA in tubular cells. Cotreatment with ADR and suPAR specifically increased the level of versican V1 in tubulointerstitial tissues and caused more obvious interstitial fibrosis in mice than treatment with only ADR.

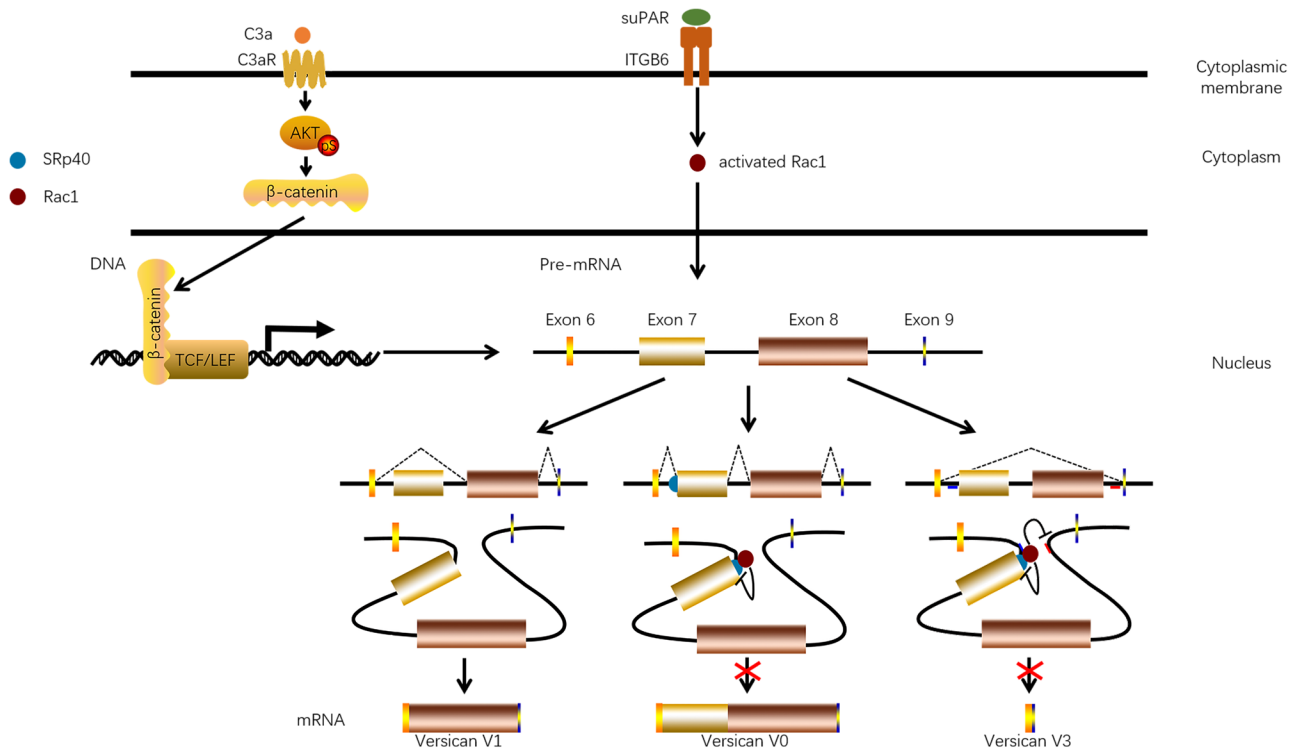


Figure 11. Schematic illustrating the role of C3a and suPAR in the formation of versican V1 in tubular cells of FSGS. C3a promotes the transcription of versican by activating the AKT/ β -catenin pathway in tubular cells. suPAR binds to ITGB6 and activates Rac1, which translocates into the nucleus and binds to SRp40 at the 5' end of exon 7 of versican pre-mRNA. This binding not only inhibits the 3'-end splicing of intron 6 but also inhibits the base-pair interaction between intron 6 and intron 8, which leads to the formation of versican V1.

Constitutive splicing includes all exons, but in versican V1, exon 7 is skipped. We explored and confirmed an SRp40 binding site at the 5' end of exon 7 of versican pre-mRNA. The SRp40 protein increases the binding of the U2 small nuclear ribonucleoprotein auxiliary factor to an upstream 3' splice site via binding to the exon (19). Markovic et al. reported that labor-induced downregulation of the splicing factor SRp40 favors the skipping of exon 12 and the upregulation of the TMD7-short corticotropin-releasing hormone receptor 1 mRNA variant (47). suPAR binds to β 3 integrin and activates the Rac1 pathway in podocytes (16). suPAR is also known to be associated with β 1 and β 2 integrins (48). We confirmed that suPAR bound to ITGB6 and activated Rac1 in the tubular cells of FSGS patients. Nuclear-translocated Rac1 bound to SRp40 and exhibited an inhibitory effect on the 3'-end splicing of intron 6. As a result, exon 7 was spliced out from versican pre-mRNA (Figure 11).

Base-pairing interactions underlie a mechanism that involves the secondary structure to regulate exon skipping (37, 49). We found a complementary interaction between introns 6 and 8 in versican pre-mRNA. The base-pairing interactions bring the 5' splice site of intron 6 into proximity with the 3' splice site of intron 8. The splicing out of both exon 7 and exon 8 leads to the formation of versican V3. An example of structure-mediated splicing is the *Drosophila* Dscam gene. The Dscam gene can potentially produce 38,016 different mRNA isoforms in *D. melanogaster*, and this process relies on competitive base pairing between the docking element and the complementary selector element of each exon cluster (50). We found that the binding site of SRp40 was close to the matching motif of versican intron 6 in tubular cells. The binding between Rac1 and SRp40 inhibited the base-pair interaction between intron 6 and intron 8, which inhibited the formation of the versican isoform V3 (Figure 11).

Although treatment with suPAR alone increased the level of versican V1 in cultured tubular cells, suPAR could not pass freely through the normal glomerular filtration barrier in vivo (20). Instead, massive amounts of suPAR passed through the glomerular filtration barrier and bound to the tubular cells in ADR-treated mice. Cotreatment with ADR and suPAR specifically increased the level of versican V1 in tubulointerstitial tissues and caused more obvious interstitial fibrosis in mice than treatment with only ADR. In addition, we analyzed the level of renal versican in patients with membranous nephropathy or minimal change disease. The mRNA levels of versican V1, V0, and V3 were all increased in the tubulointerstitial tissues of patients with membranous nephropathy, while none of the versican isoforms were increased in the tubulointerstitial tissues of patients with minimal change disease (Supplemental Figure 1). The results were consistent with previous reports that patients with FSGS showed an increase in both urine C3a and urine suPAR, while patients with membranous nephropathy showed an increase in urine C3a but not in urine suPAR; patients with minimal change disease showed neither an increase in urine C3a nor an increase in urine suPAR (9, 51). The findings support the idea that C3a and suPAR drive versican V1 expression in tubular cells and provide critical insight into the mechanism of how suPAR aggravates eGFR decline in FSGS patients.

In conclusion, our study shows that C3a and suPAR synergistically induce versican V1 expression in tubular cells by promoting transcription and splicing, respectively, and the increased tubular cell-derived versican V1 induces interstitial fibrosis by activating the CD44/Smad3 pathway in the renal fibroblasts of FSGS.

Methods

Patients and control subjects. Eight FSGS patients who underwent renal biopsies at Jingling Hospital were recruited for tubulointerstitial transcriptome analysis. The other 20 FSGS patients were enrolled for validation study. Control tissues were obtained from the unaffected portion of surgical nephrectomies, and were confirmed to be normal through light microscopy analysis. Renal specimens were kept in the Renal Biobank of National Clinical Research Center of Kidney Diseases at Jinling Hospital. Informed consent was obtained from each participant.

Isolation of tubulointerstitial tissues. For array analysis, glomeruli and the corresponding tubulointerstitium were manually separated under a stereomicroscope using 2 dissection needle holders in RNAlater at 4°C. For PCR analysis, tubulointerstitial tissues were isolated by laser capture microdissection with the Leica AS LMD System (Leica Microsystems AG). Approximately 200 cross sections were captured from each case (52).

Gene expression profile analysis. Transcriptomic analysis of microdissected tubulointerstitial tissues was performed with Affymetrix Human HTA2.0 microarrays according to standard procedures. Image generation and feature extraction were performed using Affymetrix GeneChip Command Console Software. The raw data were analyzed using the Transcriptome Analysis Console 2.0 software. The microarray data have been deposited in the NCBI's Gene Expression Omnibus (GEO GSE125779).

RT-PCR analysis. Total RNA was extracted using a RecoverAll Total Nucleic Acid Isolation Kit (AM1975, Ambion). Reverse transcription was carried out with an RT² First Strand Kit (330401, Qiagen). QuantiTect SYBR Green PCR Master Mix (204143, Qiagen) was used for gene expression level measurement. The primers for PCR analysis are listed in Supplemental Table 3.

Western blot analysis. Western blot analysis of isolated tubulointerstitial tissues or cells was performed as previously described (53, 54). Immunoprecipitation was performed with the Pierce Classic Magnetic IP/Co-IP Kit (88804, Thermo Fisher Scientific). Nuclear and cytoplasmic proteins were extracted using the NE-PER Nuclear and Cytoplasmic Extraction Kit (78833, Thermo Fisher Scientific).

Immunohistochemical staining. Paraffin-embedded sections were deparaffinized and rehydrated. Endogenous peroxidase was blocked with 0.3% hydrogen peroxide in phosphate-buffered saline (PBS) for 30 minutes. The sections were incubated for 1 hour at room temperature with primary antibody diluted in 1% BSA in PBS (Supplemental Table 4). The staining was visualized with a Polyvalent HRP/DAB detection kit (ab64264, Abcam). Negative controls were obtained by omission of the primary antibody from the staining procedure. FSP-1-positive cells in the interstitium were counted in 10 high-power fields ($\times 400$), and the indices were expressed as the mean number per field. Interstitial fibrosis was quantitatively determined with Image Pro Plus software (Media Cybernetics) in 10 high-power fields, and the interstitial fibrosis indices were expressed as the percentage blue area per field in Masson's trichrome-stained sections (55). The area of versican expression was quantified using the optical density function of the Image Pro Plus software. The average optical density was calculated by dividing the sum integrated optical density by the sum area (56).

Immunofluorescence staining. Renal sections or cultured cells were fixed with 4% paraformaldehyde. Next, the renal sections or cells were exposed to primary antibody for 2 hours before being incubated with secondary antibodies diluted in blocker for 45 minutes (Supplemental Table 4).

Culture and treatment of renal tubular cells. Immortalized tubular epithelial cells (HK-2) were cultured in DMEM/F12 medium supplemented with 10% FBS. After synchronization, cells were treated with 20% patient serum (PS), 20% heat-inactivated patient serum (HIPS), 20% healthy serum (HS), 20% heat-inactivated healthy serum (HIHS), 40 nM C3a (204881, Merck-Calbiochem), or 10 ng/ml uPAR (807-UK-100, R&D Systems). For intervention studies, 1 μ M C3aR antagonist SB290157 (559410, Merck-Calbiochem), 100 μ g/ml eculizumab (Soliris, Alexion Pharmaceuticals), 2 μ M p38 MAPK inhibitor SB203580 (559389, Merck-Calbiochem), 50 μ M ERK inhibitor PD98059 (513000, Merck-Calbiochem), and 10 μ M Akt inhibitor MK2206 (S1078, Selleck Chemicals) was given 30 minutes before treatments. Anti-uPAR blocking antibody (MAB807, R&D Systems) was preincubated at 10 μ g/ml with PS for 1 hour at 37°C before being added to cells.

CTNNB1 siRNA (sc-29209), ITGB6 siRNA (sc-43135), SRp40 siRNA (sc-38342), and Rac1 siRNA (sc-36351) were purchased from Santa Cruz Biotechnology. pENTR-N90- β -catenin and pcDNA3-EGFP-Rac1-Q61L plasmids were gifts from Xin Chen (Department of Biopharmaceutical Sciences, University of California, San Francisco, CA, USA) (Addgene plasmid 31787) and Gary Bokoch (Departments of Cell Biology and Immunology, Scripps Research Institute, La Jolla, CA, USA) (Addgene plasmid 12981) (57, 58). pGEMT-SRp40 plasmid was purchased from Sino Biological (HG16418) and His-tagged versican V3 expression plasmid was from Genecopoeia (Z6286). His-tagged versican V1 cDNA was amplified, sequenced, and subcloned into the NotI site of pcDNA3.1 plasmid (Invitrogen). Transfection of plasmids or siRNAs was conducted with Lipofectamine 2000 (Life Technologies).

Isolation of versican isoforms. To examine whether different isoforms of versican activated fibroblasts, we produced His-tagged human versican V1 and versican V3 in tubular cells and purified them on a Ni-chelate column (59). Due to its large size, we failed to clone the V0 isoform, which has a coding sequence in excess of 10 kb (60). Instead, we purified versican V0 from human medulloblastoma tissues with hyaluronan affinity chromatography as previously reported (61). The purity of isolated versican V1, V0, and V3 was verified by Western blot analysis.

Culture and treatment of renal fibroblasts. Human renal fibroblasts were purchased from Cell Biologics (H-6016) and cultured in DMEM/F12 medium supplemented with 10% FBS. After synchronization, fibroblasts were treated with the conditioned medium prepared from tubular cells (1:1 dilution) or versican (2 μ g/ml) for 48 hours. CD44 siRNA (sc-29342), ITGB1 siRNA (sc-35674), EGFR siRNA (sc-29301), PSGL1 siRNA (sc-36323) or Smad3 siRNA (sc-38376) (all Santa Cruz Biotechnology) was transfected with Lipofectamine 2000. For intervention studies, fibroblasts were preincubated with CD44 mAb (50 μ g/ml) for 15 minutes (62).

BrdU cell proliferation assay. Proliferation of renal fibroblasts was evaluated by bromodeoxyuridine (BrdU) incorporation using a commercially available BrdU ELISA kit (11647229001, Roche).

ELISA analysis of C3a and suPAR. A sandwich ELISA was performed according to the manufacturer's protocol to quantify human C3a (KA1020, Novus Biologicals), mouse C3a (NBP2-70037, Novus Biologicals), human uPAR (DY807, R&D Systems), and mouse uPAR (DY531, R&D Systems).

Animal treatment. In order to overexpress versican V1 in mouse kidneys, we administered versican V1-expressing plasmid to the mice using a previously described hydrodynamic-based gene-transfer technique (63). Briefly, we mixed versican V1-expressing plasmid (20 μ g) with approximately 2.6 ml of TransIT-EE Hydrodynamic Delivery Solution (Mirus). Then we injected the mixture into mice via the tail vein in 5 seconds. Each mouse received injections once per week for a total of 8 weeks. For interference studies, mice were treated every 7 days, intravenously with CD44 mAb (10 mg/kg) (64).

To investigate the role of C3a in the expression of versican, C3aR-knockout mice were obtained from the Jackson Laboratory (catalog 005712). C3aR-knockout and control BALB/c mice were assigned to receive a single intravenous injection of ADR (10.5 mg/kg, MilliporeSigma), and sacrificed 6 weeks after injection (65, 66). To investigate the role of suPAR in the expression of versican, suPAR (20 μ g/day) was delivered via implanting subdermal osmotic pumps (Alzet model 2006, Alza Corp.) 30 minutes before ADR treatment (7, 20). Mouse tubulointerstitial fractions were obtained from the kidney cortex using established methods adapted from Yang et al. (67).

ChIP analysis of β -catenin binding site. ChIP assay was performed with the ChIP-IT Express Magnetic Chro-

matin Immunoprecipitation kit (53008, Active Motif). The immunoprecipitations were performed with 2 μ g of antibody specific for β -catenin, or an IgG negative control at 4°C overnight with rotation. After de-cross-linking and proteinase treatment, the antibody-associated DNA fragments were amplified by PCR with primer sets that covered the β -catenin binding element on the versican promoter (Supplemental Table 3).

Luciferase assay. Cells were cotransfected with the 0.1 μ g of reporter construct (WT or mutated versican promoter–luciferase), 0.1 μ g of N90- β -catenin plasmid, and 0.02 μ g of Renilla construct. The firefly and Renilla luciferase activities were determined using the Dual-Luciferase Reporter Assay System (E1960, Promega). Values were normalized using Renilla luciferase (52).

Rac1 activation assay. Active Rac1 was measured using a G-LISA Rac1 Activation Assay Biochem kit (colorimetric assay, Cytoskeleton) as instructed by the manufacturer.

RNA-binding protein immunoprecipitation (RIP). RIP was performed using Magna RIP RNA-Binding Protein Immunoprecipitation Kit (17-700, Merk Millipore). Cells were lysed in complete RIP Lysis Buffer on ice for 5 minutes. The immunoprecipitations were performed with 5 μ g of antibodies specific for SRp40, Rac1, U2AF1, or an IgG negative control at 4°C overnight with rotation. After purification, RNA was converted into cDNA with an RT² First Strand Kit (330401, Qiagen). RT-PCR was conducted with a primer set that covered the binding element on the 5' end of versican exon 7 (Supplemental Table 3).

RNA antisense purification (RAP). To capture the intron 6/8 interaction structure that comprises versican pre-mRNA, we designed and synthesized biotinylated ssDNA oligos antisense to the RNA sequence in intron 8 of versican pre-mRNA. The target sequence did not overlap with the region that is complementary to intron 6. Cells were crosslinked with 4'-aminomethyl trioxsalen to fix endogenous RNA complexes. Crosslinked RNA was isolated using TRIzol reagent, and fragmented by incubating at 70°C for 3 minutes in Fragmentation Buffer (AM8740, Ambion). Antisense purification was performed with 2 μ g of input RNA, 15 pmol ssDNA probe, and 200 μ l streptavidin-coated magnetic beads (88816, Life Technologies) (68). After purification, RNA was converted into cDNA. PCR analysis was conducted with a primer set that covered the sequence in intron 6 of versican pre-mRNA (Supplemental Table 3).

Statistics. All of the data are expressed as the means \pm SD or medians (IQR). The data from multiple groups were analyzed with 1-way ANOVA followed by Tukey's post hoc test. Data from 2 groups were compared by a 2-tailed Student's *t* test. *P* values less than 0.05 were considered significant.

Study approval. The study was carried out in accordance with the principles of the Declaration of Helsinki and was approved by the ethics committees of Jinling Hospital. All participants provided informed consent. Animals used in this study were approved by the Institutional Animal Care and Use Committee of Jinling Hospital.

Author contributions

HB and ZL designed the study. RH, SH, WQ, QH, XW, XX, MZ, and CZ performed the experiments. JS performed data bioinformatics analysis. RH, HB, and ZL wrote the manuscript. ZL and HB are the guarantors of this work and, as such, had full access to all the data in the study and take responsibility for the integrity of the data and the accuracy of the data analysis. All authors read and approved the final version of manuscript.

Acknowledgments

We thank the physicians, patients, and volunteers who contributed to this study. This work is supported by grants from the National Natural Science Foundation of China (81873610, 81200516), the Natural Science Foundation of Jiangsu Province (BK20171330, BK2012372), the Deng Feng Scholars of Nanjing University (2015-105), the Fundamental Research Funds for the Central Universities (021414380347), the National Key Research and Development Program of China (2016YFC0904100), the Major International (Regional) Joint Research Project (81320108007), and the Key Research and Development Program of Jiangsu Province (BE2016747).

Address correspondence to: Hao Bao or Zhihong Liu, Southeast University School of Medicine, National Clinical Research Center of Kidney Diseases, Jinling Hospital, Nanjing 210002, China; National Clinical Research Center of Kidney Diseases, Jinling Hospital, Nanjing University School of Medicine, Nanjing 210002, China. Phone: 86.25.84801992; Email: bhao@nju.edu.cn (H. Bao); zhihong-liu@hotmail.com (Z. Liu).

1. D'Agati VD, Kaskel FJ, Falk RJ. Focal segmental glomerulosclerosis. *N Engl J Med.* 2011;365(25):2398–2411.
2. Tang X, Xu F, Chen DM, Zeng CH, Liu ZH. The clinical course and long-term outcome of primary focal segmental glomerulosclerosis in Chinese adults. *Clin Nephrol.* 2013;80(2):130–139.
3. Alexopoulos E, Stangou M, Papagianni A, Pantzaki A, Papadimitriou M. Factors influencing the course and the response to treatment in primary focal segmental glomerulosclerosis. *Nephrol Dial Transplant.* 2000;15(9):1348–1356.
4. Bukong TN, Maurice SB, Chahal B, Schaeffer DF, Winwood PJ. Versican: a novel modulator of hepatic fibrosis. *Lab Invest.* 2016;96(3):361–374.
5. Rienstra H, et al. Differential expression of proteoglycans in tissue remodeling and lymphangiogenesis after experimental renal transplantation in rats. *PLoS One.* 2010;5(2):e9095.
6. Camussi G, et al. In vivo localization of C3 on the brush border of proximal tubules of kidneys from nephrotic patients. *Clin Nephrol.* 1985;23(3):134–141.
7. Hahm E, et al. Bone marrow-derived immature myeloid cells are a main source of circulating suPAR contributing to proteinuric kidney disease. *Nat Med.* 2017;23(1):100–106.
8. Hayek SS, et al. Soluble urokinase receptor and chronic kidney disease. *N Engl J Med.* 2015;373(20):1916–1925.
9. Huang J, et al. Urinary soluble urokinase receptor levels are elevated and pathogenic in patients with primary focal segmental glomerulosclerosis. *BMC Med.* 2014;12:81.
10. Rudnicki M, et al. Increased renal versican expression is associated with progression of chronic kidney disease. *PLoS ONE.* 2012;7(9):e44891.
11. Wu YJ, La Pierre DP, Wu J, Yee AJ, Yang BB. The interaction of versican with its binding partners. *Cell Res.* 2005;15(7):483–494.
12. Gu H, et al. Crosstalk between TGF- β 1 and complement activation augments epithelial injury in pulmonary fibrosis. *FASEB J.* 2014;28(10):4223–4234.
13. Zhu Y, et al. Klotho suppresses tumor progression via inhibiting PI3K/Akt/GSK3 β /Snail signaling in renal cell carcinoma. *Cancer Sci.* 2013;104(6):663–671.
14. Zhang X, et al. Regulation of Toll-like receptor-mediated inflammatory response by complement in vivo. *Blood.* 2007;110(1):228–236.
15. Ahamed J, Venkatesha RT, Thangam EB, Ali H. C3a enhances nerve growth factor-induced NFAT activation and chemokine production in a human mast cell line, HMC-1. *J Immunol.* 2004;172(11):6961–6968.
16. Wei C, et al. Modification of kidney barrier function by the urokinase receptor. *Nat Med.* 2008;14(1):55–63.
17. Wei C, et al. Circulating urokinase receptor as a cause of focal segmental glomerulosclerosis. *Nat Med.* 2011;17(8):952–960.
18. Piva F, Giuliotti M, Burini AB, Principato G. SpliceAid 2: a database of human splicing factors expression data and RNA target motifs. *Hum Mutat.* 2012;33(1):81–85.
19. Yan XB, et al. Alternative splicing in exon 9 of glucocorticoid receptor pre-mRNA is regulated by SRp40. *Mol Biol Rep.* 2010;37(3):1427–1433.
20. Cathelin D, et al. Administration of recombinant soluble urokinase receptor per se is not sufficient to induce podocyte alterations and proteinuria in mice. *J Am Soc Nephrol.* 2014;25(8):1662–1668.
21. Venkatesan N, et al. Glycosyltransferases and glycosaminoglycans in bleomycin and transforming growth factor- β 1-induced pulmonary fibrosis. *Am J Respir Cell Mol Biol.* 2014;50(3):583–594.
22. Einecke G, et al. A molecular classifier for predicting future graft loss in late kidney transplant biopsies. *J Clin Invest.* 2010;120(6):1862–1872.
23. Roy-Chaudhury P, et al. CD44 in glomerulonephritis: expression in human renal biopsies, the Thy 1.1 model, and by cultured mesangial cells. *Kidney Int.* 1996;50(1):272–281.
24. Rouschop KM, et al. CD44 deficiency increases tubular damage but reduces renal fibrosis in obstructive nephropathy. *J Am Soc Nephrol.* 2004;15(3):674–686.
25. Chen CH, et al. Oligo-fucoidan prevents renal tubulointerstitial fibrosis by inhibiting the CD44 signal pathway. *Sci Rep.* 2017;7:40183.
26. Li Y, et al. Severe lung fibrosis requires an invasive fibroblast phenotype regulated by hyaluronan and CD44. *J Exp Med.* 2011;208(7):1459–1471.
27. Mathern DR, Heeger PS. Molecules great and small: the complement system. *Clin J Am Soc Nephrol.* 2015;10(9):1636–1650.
28. Peng Q, et al. C3a and C5a promote renal ischemia-reperfusion injury. *J Am Soc Nephrol.* 2012;23(9):1474–1485.
29. Buelli S, et al. Protein load impairs factor H binding promoting complement-dependent dysfunction of proximal tubular cells. *Kidney Int.* 2009;75(10):1050–1059.
30. Zaferani A, et al. Identification of tubular heparan sulfate as a docking platform for the alternative complement component properdin in proteinuric renal disease. *J Biol Chem.* 2011;286(7):5359–5367.
31. Liu J, et al. Serum C3 and renal outcome in patients with primary focal segmental glomerulosclerosis. *Sci Rep.* 2017;7(1):4095.
32. Wang F, Li X, Zhu X, Chen Q, Jiang L, Zhu Z. Renal tubular complement 3 deposition in children with primary nephrotic syndrome. *Biomed Res Int.* 2018;2018:4386438.
33. Tang Z, Lu B, Hatch E, Sacks SH, Sheerin NS. C3a mediates epithelial-to-mesenchymal transition in proteinuric nephropathy. *J Am Soc Nephrol.* 2009;20(3):593–603.
34. Cai T, et al. FHL2 promotes tubular epithelial-to-mesenchymal transition through modulating β -catenin signalling. *J Cell Mol Med.* 2018;22(3):1684–1695.
35. Fang D, et al. Phosphorylation of beta-catenin by AKT promotes beta-catenin transcriptional activity. *J Biol Chem.* 2007;282(15):11221–11229.
36. Rahmani M, et al. Regulation of the versican promoter by the beta-catenin-T-cell factor complex in vascular smooth muscle cells. *J Biol Chem.* 2005;280(13):13019–13028.
37. Lin CL, Taggart AJ, Fairbrother WG. RNA structure in splicing: An evolutionary perspective. *RNA Biol.* 2016;13(9):766–771.
38. Zhao X, Russell P. Versican splice variants in human trabecular meshwork and ciliary muscle. *Mol Vis.* 2005;11:603–608.
39. Foulcer SJ, Day AJ, Apte SS. Isolation and purification of versican and analysis of versican proteolysis. *Methods Mol Biol.*

- 2015;1229:587–604.
40. Sheng W, et al. The roles of versican V1 and V2 isoforms in cell proliferation and apoptosis. *Mol Biol Cell*. 2005;16(3):1330–1340.
 41. Wu Y, et al. Versican V1 isoform induces neuronal differentiation and promotes neurite outgrowth. *Mol Biol Cell*. 2004;15(5):2093–2104.
 42. Smith HW, Marshall CJ. Regulation of cell signalling by uPAR. *Nat Rev Mol Cell Biol*. 2010;11(1):23–36.
 43. Blasi F, Carmeliet P. uPAR: a versatile signalling orchestrator. *Nat Rev Mol Cell Biol*. 2002;3(12):932–943.
 44. Spinale JM, et al. A reassessment of soluble urokinase-type plasminogen activator receptor in glomerular disease. *Kidney Int*. 2015;87(3):564–574.
 45. Sinha A, et al. Serum-soluble urokinase receptor levels do not distinguish focal segmental glomerulosclerosis from other causes of nephrotic syndrome in children. *Kidney Int*. 2014;85(3):649–658.
 46. Saleem MA. What is the role of soluble urokinase-type plasminogen activator in renal disease? *Nephron*. 2018;139(4):334–341.
 47. Markovic D, Grammatopoulos DK. Focus on the splicing of secretin GPCRs transmembrane-domain 7. *Trends Biochem Sci*. 2009;34(9):443–452.
 48. Selleri C, et al. In vivo activity of the cleaved form of soluble urokinase receptor: a new hematopoietic stem/progenitor cell mobilizer. *Cancer Res*. 2006;66(22):10885–10890.
 49. Miriami E, Margalit H, Sperling R. Conserved sequence elements associated with exon skipping. *Nucleic Acids Res*. 2003;31(7):1974–1983.
 50. Yang Y, et al. RNA secondary structure in mutually exclusive splicing. *Nat Struct Mol Biol*. 2011;18(2):159–168.
 51. Morita Y, Ikeguchi H, Nakamura J, Hotta N, Yuzawa Y, Matsuo S. Complement activation products in the urine from proteinuric patients. *J Am Soc Nephrol*. 2000;11(4):700–707.
 52. Bao H, et al. MiR-223 downregulation promotes glomerular endothelial cell activation by upregulating importin $\alpha 4$ and $\alpha 5$ in IgA nephropathy. *Kidney Int*. 2014;85(3):624–635.
 53. Bao H, Ge Y, Zhuang S, Dworkin LD, Liu Z, Gong R. Inhibition of glycogen synthase kinase-3 β prevents NSAID-induced acute kidney injury. *Kidney Int*. 2012;81(7):662–673.
 54. Kischel P, et al. Versican overexpression in human breast cancer lesions: known and new isoforms for stromal tumor targeting. *Int J Cancer*. 2010;126(3):640–650.
 55. Inoue T, Suzuki H, Okada H. Targeted expression of a pan-caspase inhibitor in tubular epithelium attenuates interstitial inflammation and fibrogenesis in nephritic but not nephrotic mice. *Kidney Int*. 2012;82(9):980–989.
 56. Ritter CS, Finch JL, Slatopolsky EA, Brown AJ. Parathyroid hyperplasia in uremic rats precedes down-regulation of the calcium receptor. *Kidney Int*. 2001;60(5):1737–1744.
 57. Tward AD, et al. Distinct pathways of genomic progression to benign and malignant tumors of the liver. *Proc Natl Acad Sci USA*. 2007;104(37):14771–14776.
 58. Subauste MC, et al. Rho family proteins modulate rapid apoptosis induced by cytotoxic T lymphocytes and Fas. *J Biol Chem*. 2000;275(13):9725–9733.
 59. Kim S, et al. Carcinoma-produced factors activate myeloid cells through TLR2 to stimulate metastasis. *Nature*. 2009;457(7225):102–106.
 60. Fang L, et al. Versican 3'-untranslated region (3'-UTR) functions as a ceRNA in inducing the development of hepatocellular carcinoma by regulating miRNA activity. *FASEB J*. 2013;27(3):907–919.
 61. Dutt S, Kléber M, Matasci M, Sommer L, Zimmermann DR. Versican V0 and V1 guide migratory neural crest cells. *J Biol Chem*. 2006;281(17):12123–12131.
 62. Zhang S, et al. Targeting chronic lymphocytic leukemia cells with a humanized monoclonal antibody specific for CD44. *Proc Natl Acad Sci USA*. 2013;110(15):6127–6132.
 63. Meng J, et al. MicroRNA-196a/b mitigate renal fibrosis by targeting TGF- β receptor 2. *J Am Soc Nephrol*. 2016;27(10):3006–3021.
 64. Weigand S, et al. Global quantitative phosphoproteome analysis of human tumor xenografts treated with a CD44 antagonist. *Cancer Res*. 2012;72(17):4329–4339.
 65. Li J, Campanale NV, Liang RJ, Deane JA, Bertram JF, Ricardo SD. Inhibition of p38 mitogen-activated protein kinase and transforming growth factor-beta1/Smad signaling pathways modulates the development of fibrosis in Adriamycin-induced nephropathy. *Am J Pathol*. 2006;169(5):1527–1540.
 66. Wang Y, Wang YP, Tay YC, Harris DC. Progressive Adriamycin nephropathy in mice: sequence of histologic and immunohistochemical events. *Kidney Int*. 2000;58(4):1797–1804.
 67. Yang L, Besschetnova TY, Brooks CR, Shah JV, Bonventre JV. Epithelial cell cycle arrest in G2/M mediates kidney fibrosis after injury. *Nat Med*. 2010;16(5):535–543.
 68. Engreitz JM, et al. RNA-RNA interactions enable specific targeting of noncoding RNAs to nascent pre-mRNAs and chromatin sites. *Cell*. 2014;159(1):188–199.